Article

Not peer-reviewed version

Paleoenvironmental reconstruction of Lake Vrana on the Island of Cres (Croatia) based on geochemistry and mineralogy of the Late Pleistocene and Holocene sediments

Nikolina Ilijanić , Slobodan Miko , Ozren Hasan , Dea Brunović , Martina Šparica Miko , Saša Mesić *

Posted Date: 29 August 2024

doi: 10.20944/preprints202408.2193.v1

Keywords: karst lake; lake sediments; geochemistry; mineralogy, Late Pleistocene, Holocene, eastern Adriatic coast

 doi:10.20944/preprints202408.2193.v1

Article

Paleoenvironmental Reconstruction of Lake Vrana on the Island of Cres (Croatia) Based on Geochemistry and Mineralogy of the Late Pleistocene and Holocene Sediments

Nikolina Ilijanić, Slobodan Miko, Ozren Hasan, Dea Brunović, Martina Šparica Miko and Saša Mesić *

Croatian Geological Survey, Sachsova 2, 10000 Zagreb, Croatia
* Correspondence: smesic@hgi-cgs.hr

Abstract: A 7.4 m long sediment core has been retrieved from the central part of Lake Vrana on the Island of Cres to reconstruct the paleoenvironmental conditions. Lake Vrana is the deepest freshwater lake in Croatia, located in the karst region of the eastern Adriatic coast. A dated sediment sequence in Lake Vrana of 4.4 m spans the past 16.4 kyr, and features a dynamic sediment deposition until the beginning of the Holocene, including strong sediment input and supply to the lake by runoff sediments of dolomitic origin from the catchment in the period 16.4-14.4 cal kyr BP. High organic carbon content, which originates from mixed terrestrial and aquatic origins in the periods 14.4-13.3 cal kyr BP and 12.7-11.7 cal kyr BP, indicates fluctuating lake levels in shallow water environments during the late glacial to Holocene transition. The Holocene sequence indicates the development of more stable conditions and continuous sediment deposition, characterized by increasing trend of siliciclastic sediments delivered into the lake during the early Holocene (11.7-10 cal kyr BP), and dominantly from 8 to 4.4 cal kyr BP, indicating enhanced input and erosion, which coincides with humid and pluvial period, recorded in the central Mediterranean region. It is followed by sediments with high organic carbon content between 4.4 to 1.6 cal kyr BP, which points to higher lake productivity. Calcite sedimentation prevail between 1.6 to 0.4 cal kyr BP, indicating stable deeper-lake conditions, while dominantly siliciclastic sediments in the period 0.4-0.1 cal kyr BP indicate erosion during Little Ice Age (LIA), with enhanced precipitation and sediment discharge from the catchment. The re-establishment of calcite sedimentation has been observed over the last 100 years.

Keywords: karst lake; lake sediments; geochemistry; mineralogy; late Pleistocene; Holocene; eastern Adriatic coast

1. Introduction

Coastal karst lakes are widespread in the Mediterranean region [1]. Lake Vrana is a coastal lake, due to its location in the central part of the Island of Cres, in the northern part of the eastern Adriatic coast, central Mediterranean. Although only between 3 to 6 km away from the sea on each side, the sea has no influence on lake water chemistry [2,3]. This unique hydrological and hydrogeological system has allowed continuous water pumping from the lake for water supply since the middle of the 20th century and is active today [4]. Therefore, it is prone to vulnerability, and its limnological characteristics and paleolimnological study of lake sediments play an important role in its preservation and protection from anthropogenic influences.

Lake sediments provide opportunities to reconstruct past aquatic ecosystems [5]. Evaluating the stored environmental information in sediments depends on the knowledge of the ecosystem and the understanding of the present-day lake response to environmental variability. Lake sediments are the

 doi:10.20944/preprints202408.2193.v1

result of input of the material from the catchment and the lake productivity itself [6]. The terrestrial input to the lake is carried through erosional processes and anthropogenic paths. Knowledge of the processes driving terrestrial input is essential to understanding carbon deposition and nutrient input, which are linked to climate through weathering and transport processes. However, understanding anthropogenic impacts is key to assessing the environmental status of a lake today and in recent history. Depositional environmental changes have been studied in karstic lakes [7–11], wetlands [12], and paleolakes and present-day karstic poljes [13,14]. Important sedimentary archives are submerged paleolakes and present-day marine channels [15–18], submerged sinkholes [19–23], and submerged estuaries [24–26] in the eastern Adriatic coast. In carbonate bedrock, karstic processes, such as dissolution and collapse, are very effective in creating drainage patterns and depressions for lake development, which leads to the formation of water-filled dolines [27]. Calcium and carbonate dominate sediments in calcareous regions [6]. The development of lakes on limestone substrates favors carbonate-rich waters; therefore, karstic freshwater lakes are subject to endogenic (authigenic) carbonate production (lake carbonate marls) during dry summer periods, triggered by aquatic productivity. The key compositional properties for the karstic area are carbonate, siliciclastic, and organic materials used to reconstruct environmental changes. Through lake sediment geochemical stratigraphy, it is possible to infer environmental changes and basin development. In Lake Vrana sediments, the environmental geochemical distribution and tracing of the history of anthropogenic and atmospheric Pb pollution have already been conducted [28,29], comparing the lake sediments to the catchment soils and discriminating anthropogenic from geogenic sources of Pb.

The coastline of the eastern Adriatic region was affected by sea-level changes during the late Pleistocene and Holocene. In general, the mean global sea level from 120,000 years ago was comparable to the present one, while during the Last Glacial Maximum (LGM) period, the sea level was 120-130 m lower than today [30–32], and vast areas between the islands were dry land. It is considered that most of the basins were drowned after the LGM sea-level rise [33], but this may not be the case for the inland basins within the islands, and their exact evolution is yet to be determined.

In this study, we aimed to utilize the geochemical and mineralogical (bulk and clay minerals) signatures of lake sediments in Lake Vrana on the Island of Cres to constrain the paleoenvironmental evolution of the lake and possibly identify sediment sources. To document this, we investigated the geochemical and mineral composition of lake sediments and soil profiles in comparison with those from local sources collected near the study site. This allowed the identification of fine-grained terrigenous material in lake sediments from different provenances, and thus allowed the exploration of the link between clay mineral assemblages and paleoenvironmental changes. Lake development is considered to be closely connected to vegetation changes using pollen in Lake Vrana [7] from the late glacial period and the record of lake-level dynamics using diatoms in the last 2200 years [9]. The main aspects considered in the present work are lake evolution under the light of sedimentary, geochemical, and mineralogical processes in relation to sea level rise and the association between limnological evolution and paleohydrological changes.

2. Materials and Methods

2.1. Site Description

Lake Vrana is a karst lake on the island of Cres, located in the Kvarner region in the northern part of the Adriatic Sea (Figure 1). The island of Cres is one of the largest and highest islands on the Croatian coast, with an area of 405.7 km^2, a coastline length of 268.2 km, and the highest peak of 648 m [34]. The highest area on the Island of Cres is located in the northern part of the island, which is the narrowest. Prehistoric hillforts exist on the island heights, most of which are located in the central part of the island. They represent evidence of human settlements in the past, from the pre-Roman period. Lake Vrana is located in the middle of the island and is elongated in the NW-SE direction, following the extension of the island in the same direction (Dinaric strike). The lake is 5.5 km long and 1.45 km wide. The surface of the lake is 5.75 km^2, while the surficial catchment area is 38 km^2 (defined by ArcGIS from a 25 m resolution digital elevation model). The lake is a crypto-depression

 doi:10.20944/preprints202408.2193.v1

with an average altitude of the mean lake level of 12.78 m a.s.l. [2,35]. The water-level oscillations in the period 1929-2019 range between 9.11 m a.s.l. and 15.93 m a.s.l. (avg. 13-16 m a.s.l.), but in the period 1985-2019 the average lake-water level was 11-12 m a.s.l. [35]. The lake water volume is 220 million cubic meters. The bottom of the lake is mostly flat, with an average water depth of 54-55 m (41-42 m b.s.l.). The deepest part of the lake is a 74.5 m (61.3 m b.s.l.) deep conical depression in the SW part of the lake. The depression is approximately 250 m wide, and is interpreted as a collapsed sinkhole filled with sediments.

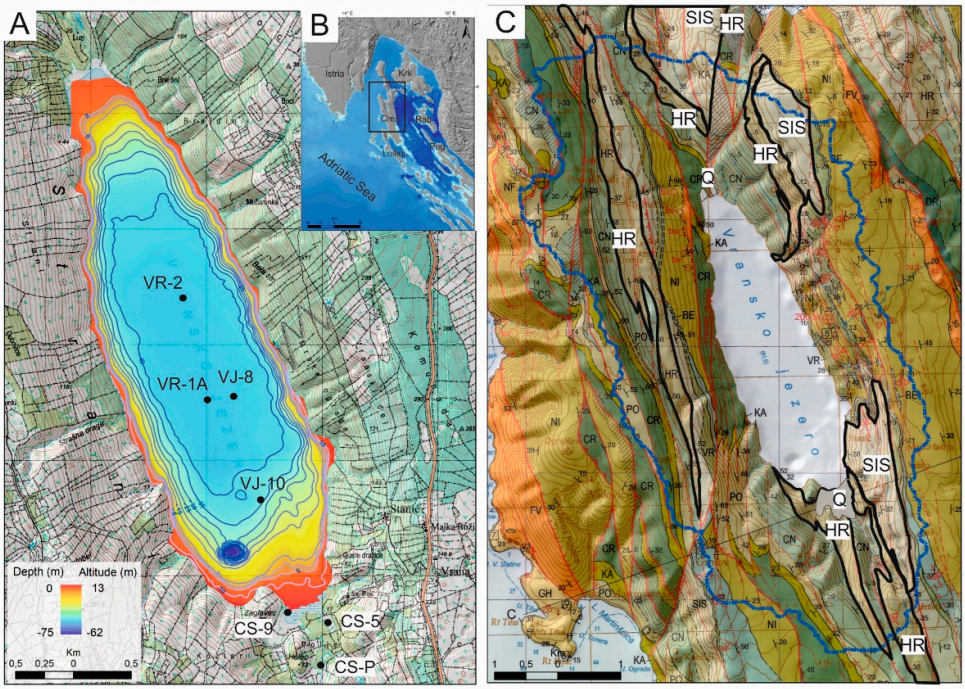

Figure 1. A. Bathymetry map of Lake Vrana on the Island of Cres (in absolute depths), with the location of sediment cores (VR-1A, VR-2, VJ-8, VJ-10, CS-5, CS-9, CS-P). B. Location of Lake Vrana in the northern part of the Adriatic Sea. C. A geological map of Lake Vrana (modified from 36). The surficial catchment area is outlined in a blue line, and Quaternary sediments (Q) are marked in gray on the northern and southern shores of the lake. Geological units with dolomite (SIS, HR) are highlighted with black lines. Geological lithostratigraphic units shown on the map: DR-Valanginian to Hauterivian micrite Dragozetići limestones; CR-Upper Hauterivian to Barremian Cres limestones, dolomites, stromatolites, breccias and emerged surface alterations; KA-Aptian Kanfanar limestones; PO-Upper Aptian- Lower Albian Porozina breccia and limestones; CN-Albian Crna limestones with emersion breccias; HR-Upper Albian Hrasta dolomites; SIS-Upper Albian-Lower Cenomanian alteration of Sis dolomites and limestones with relict stromatolites, breccia and bauxite infillings; VR-Lower Cenomanian Vrana limestones; BE-Lower to Middle Cenomanian Belej pelagic limestones; NI-Cenomanian Niska limestones; SD-Upper Cenomanian to Turonian Sveti Duh pelagic limestones; GH-Turonian to Coniacian Gornji Humac limestones; FV-Lower to Mid Eocene foraminiferal limestones [36].

The Island of Cres is part of the Adriatic Carbonate Platform [37,38]. It is mostly composed of karstified carbonate rocks: Upper Cretaceous rudist limestones, Eocene limestones, dolomites, and Paleogene flysch deposits [36] (Figure 1C). In the Late Cretaceous the final disintegration of the Adriatic carbonate platform began and culminated during the Neogene (Oligocene-Miocene) when Dinarides were formed. Lake Vrana is situated within the top of a reversibly uplifted and tectonically disturbed anticline in the northeast-southwest orientation of Dinarides. Lake Vrana is predefined by a northwest-southeast striking tectonic fault where dolomites occur [2]. Dolomite rocks form the core of the anticline. They lie beneath the sediments of Lake Vrana, and have a strong influence on lake formation. Dolomites prevail over limestones in the immediate catchment of Lake Vrana. The dolomite-rich geological lithostratigraphic units (Upper Albian-Lower Cenomanian alteration of Sis

 doi:10.20944/preprints202408.2193.v1

dolomites and limestones-SIS unit) and Upper Albian Hrasta dolomites-HR unit) are present on the southern and northern shores [36]. The units are elongated in the lake direction. Quaternary deposits are of limited extent and are represented by breccias, alluvial and colluvial deposits, and eolian sediments. Fine-grained Quaternary lake sediments are identified and mapped on the northern and southern shores of the lake. Lake Vrana is considered to be of Late Pleistocene origin, developed as a karstic depression filled with Quaternary sediments, and their thickness in the central part of the lake, recorded by seismic acoustics, is more than 25 m [7].

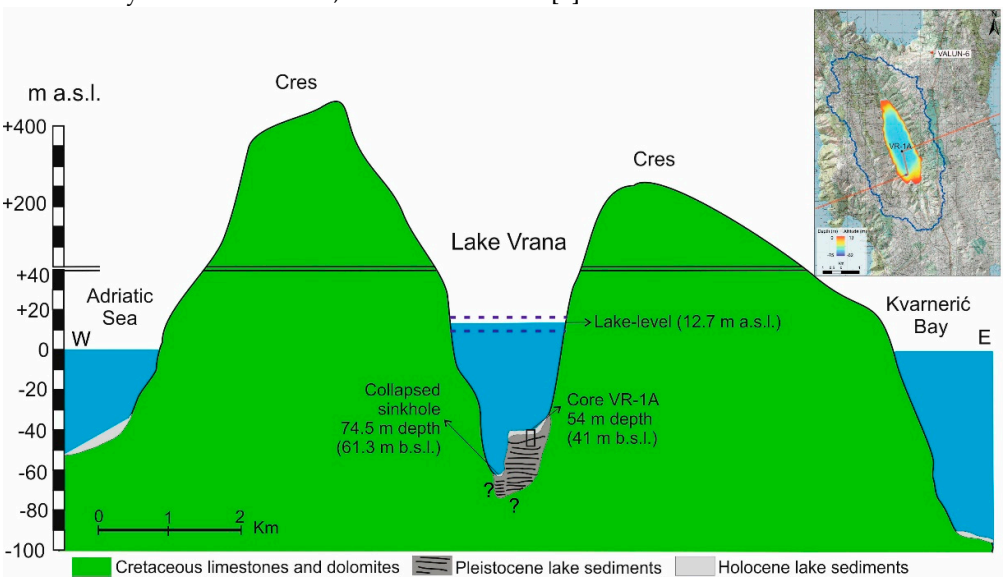

Figure 2. Schematic overview of the Lake Vrana on the Island of Cres, in the profile (red line on the map) from the collapsed sinkhole and projected sediment core VR-1A (both not to scale). The dotted blue lines represent the average lake level (12.7 m a.s.l.), the lowest lake level (9 m a.s.l.), and the highest lake level (16 m a.s.l.). Sample VALUN-6 outside of the catchment is marked on the small map.

The lake is situated in the central part of the Island of Cres, 3.4 km and 4 km from the sea on the western and eastern sides, respectively. On the NW side, the sea is 3.1 km distant and on the SW side, it is almost 6 km. Although the lake is close to the sea, there is no connection to seawater, neither through the surface nor the karstic underground. Lake Vrana receives water predominantly through precipitation, and through groundwater to a lesser extent [2,39]. Therefore, the lake recharge is from its catchment area of nearly 33 km^2, and 33% of the recharge is from precipitation on the lake surface [2]. It has no permanent surface or underground inflows or outflows and is a closed lake type. Streams and flood flows/surges occur during rainy periods. They mainly feed the lake and are formed on the steep shores on the western and eastern sides, as well as on the northern and southern shores of the lake. Total freshwater seasonal inflows and precipitation have sufficient capacity to maintain a relatively stable level in Lake Vrana. Therefore, the variability of the lake level corresponds to annual precipitation changes, which directly depend on variability during the winter season [2,35]. Lake discharge occurs mainly through evapotranspiration during the summer months and possibly through the karst underground [2,35]. It is not detected in the submarine spring (vrulja) Valun north of the lake but could be detected in vrulja Vrutek, on the western shores of the Island of Cres [2,35]. The annual evaporation rate from the lake surface is 1161 mm [2]. The proposed average water residence time in the lake is 32 years [2,40]. The water level oscillated on average from 13-16 m a.s.l. in the period 1929-2019, but in the period 1985-2019 the average lake-water level decreased, on average to 11-12 m a.s.l., with no significant decrease in precipitation [35]. Lake Vrana is a reservoir of freshwater used for public water supply since the middle of the 20th century. The possible effects of increasing water consumption from the lake due to the extraction of the public water supply have been investigated in terms of seasonal temperature variations in air and water temperatures, precipitation, and water level [2,35] as well as future predictions [4,41]. After the mid-1980s, the mean

 doi:10.20944/preprints202408.2193.v1

water level decreased, culminating in 1990 with a 4 m anthropic low water level (up to 9.11 m a.s.l.), which most probably occurred due to both, hydraulic water pumping and a slight decrease in precipitation [2,42]. The amount of abstracted water rose significantly from the mid to the end of the 20th century due to the increasing demand for water on the Island of Cres and surrounding islands, especially due to tourism in the summer months when the consumption of water significantly increases [35].

The average annual air temperature on the island Cres is 14.3°C, and the average annual precipitation is 1054 mm, with the lowest precipitation between April and September (from 1961 to 1990, meteorological station Cres; 2). The whole island is exposed to the northeastern wind bora, especially in the southern part of the lake catchments where the vegetation is low and degraded, with bare karst relief on the surface.

Limnological measurements of Lake Vrana have shown that the lake is an oligotrophic, hard-water lake, mixed once a year during the winter months. It is a monomictic lake, characterized by a thermal stratification event in spring, after winter isothermal conditions below 8°C [2]. During the summer, thermal stratification was established at a depth of 10–20 m. The mean temperature of the summer epilimnion (from the surface to the 10 m water column depth) is 25°C, and the hypolimnion temperature at a depth of 20–70 m is 7°C [2]. Estimation of the lake surface water temperature (at a water depth of approximately 0.3 m) based on air temperature using support vector regression predicts an increase of an average of 1.2°C over the next 50 years [41].

Lake water geochemical parameters measured at two locations up to 50 m depth from the central part of the lake, are characterized by calcium (Ca^{2+}=54 mg/l) and bicarbonate ions (HCO_3^- =180-188 mg/l). The lake has slightly alkaline waters, pH varies between 6 and 8 in the water column. The dissolved oxygen concentration in Lake Vrana is approximately 10 mg/l under isothermal conditions, while the vertical stratification of dissolved oxygen ranges between 8-10 mg/l in the epilimnion to approximately 6 mg/l in the hypolimnion [3]. The influence of sea water is negligible, as evidenced only by small amounts of chloride ions (Cl- =30-62 mg/l), due to the wind-borne sea spray on the surface of the lake. Electrical conductivity (EC), total dissolved salts (TDS) and nitrogen ions (NO_3) are also very low, 423-439 μS/cm, 284-295 mg/l and 0.1-1.5 mg/l, respectively [43], and belongs to oligotrophic lakes [3].

The phytoplankton community of Lake Vrana comprises diatoms (*Bacillariophyta*), chrysophytes (*Chrysophyceae*), and dinoflagellates (*Dinophyceae*), which are the most diverse and abundant groups recorded in other karstic lakes along the Dalmatian coast [44,45]. The distribution of macrophytic vegetation present at the bottom of Lake Vrana is divided into shallow water vegetation in the northern and southern parts dominated by reeds and rush, followed by the sedge zone and submerged vegetation species of spawners. Such vegetation is widespread up to a depth of 7 m, where it is replaced by stonewarts or charophytes (up to 30 m in depth), which is the most widespread vegetation in Lake Vrana [46,47].

2.2. Sediment Sampling

In 2010, a 7.42 m-long sediment core VR-1A and 5.45 m-long parallel sediment core VR-1 were retrieved from the center of the Lake Vrana at water depth of 54 m (41 m b.s.l.) (Figure 1). Additionally, 370 m to the north, two sediment cores were extracted, 5.69 m long sediment core VR-2 and parallel VR-2A (1.50-4.28 m). The cores were retrieved using a piston corer mounted on a tripod tower and rope-operated on a floating platform (UWITEC, Austria). The sediment cores were cored by hammering with a stainless-steel liner from the platform, and were collected in 3-m long sections of plastic liners, 60 mm in diameter.

Sediment core VR-1A was used in this study, whereas the others were archived in a cooling chamber for future analysis. The sediment core obtained by piston coring could have been disturbed in the upper part when piston reached the soft lake sediments at the surface of the lake bottom. Therefore, the short sediment cores VJ-8 (0-0.92 m) and VJ-10 (0-0.74 m) were taken in 0.90 m-long plastic liners (12 cm in diameter) by scuba-diving and simple pressing into the soft sediment at 53.5 m and 48 m depth, respectively (Figures 1 and 3). Sediment core VJ-8 is located close to the long core

 doi:10.20944/preprints202408.2193.v1

VR-1A (212 m away), while core VJ-10 is located further south, but also on the flat lake bottom, 920 m away from VJ-8.

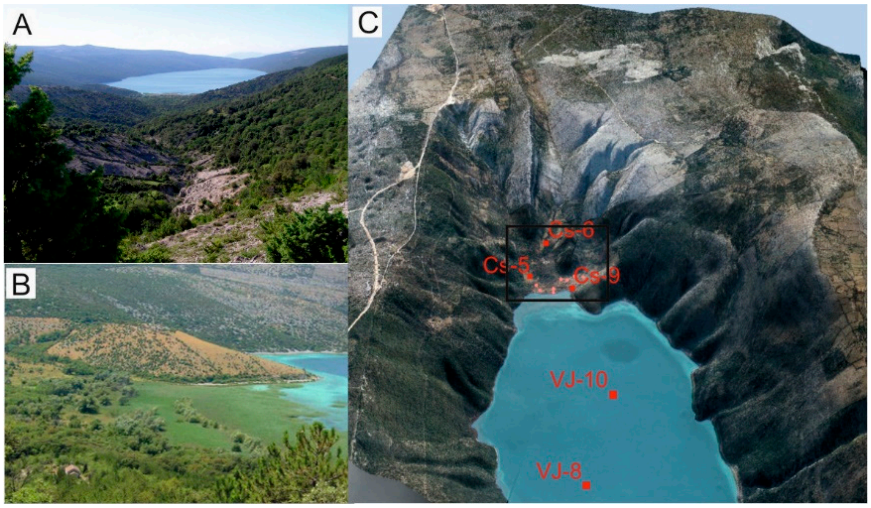

Figure 3. A. View of the Lake Vrana from the south. B. Alluvial fan in the southern shores of Lake Vrana, where sediment cores CS-5 and 9 were taken, marked in black rectangle (C). C. Areal images of the southern shore of Lake Vrana, with marked sediment cores in the alluvial fan and short cores (VJ-8 and VJ-10). Note the bare karst relief on the southern part of the lake catchment.

As Lake Vrana is elongated in the NNW-SSE direction, it is characterized by steep lake shores on both sides, while the northern and southern shores show gentle relief. Moreover, the southern shores of the lake are characterized by the appearance of alluvial fans, where the material is carried by streams and flood flows, where canyon-type channels have been developed. In one such bed of an occasional stream, at ca. 25 m a.s.l, a CS-P soil profile was sampled (Figure 3). The profile is composed of colluvium (sediment formed by gravitational erosion at higher elevations by streams). It was sampled as an outcrop, at intervals of 2 cm. The profile can be divided into the upper brown dolomitized soil down to ~40 cm, followed by a soil layer with pottery fragments (1.70-1.88 m). Lower brown soil follows down to 2.28 m, where the transition to yellowish fine-grained sediments begins, similar to loess (loess-like sediments). Loess-like sediments extend to the end of the profile, that is, 3.40 m.

Further north of the soil profile CS-P, closer to the lake, CS-5 and CS-9 sediment cores were drilled using Eijkelkamp percussion drilling equipment (Cobra TT), using 1-m extension rods and stainless-steel liner, 10 cm in diameter. Extracted sediment cores were sectioned carefully at 2-cm, 5-cm, or 10-cm intervals during the sampling, wrapped in plastic bags, and transported to the laboratory. The sediment core CS-5 (0-5.19 m) was located in an alluvial fan, at 15.5 m a.s.l., and is a continuation of the intermittent stream, from which the CS-P profile was sampled. The sediments from CS-5 were composed of red soil. Sediment core CS-9 (0-5.51 m) is located in the top part of the alluvial fan and forms a flood deposit along the edge of the lake, at 13.1 m a.s.l. Sediments from the CS-9 core consist of eroded dolomite rock in the upper part and eroded soil in the lower part of the core.

In the northwestern part of the lake in the large paleo-depression next to the Valun Cres road, soil samples were taken to a depth of 9.30 m. A representative sample (VALUN-6) was used in this study. Although the location of the VALUN-6 sample was outside the boundaries of the surface catchment (Figure 2), it was included in the study because such material-terra rossa/red soil could also be the source material of sediments in the lake.

 doi:10.20944/preprints202408.2193.v1

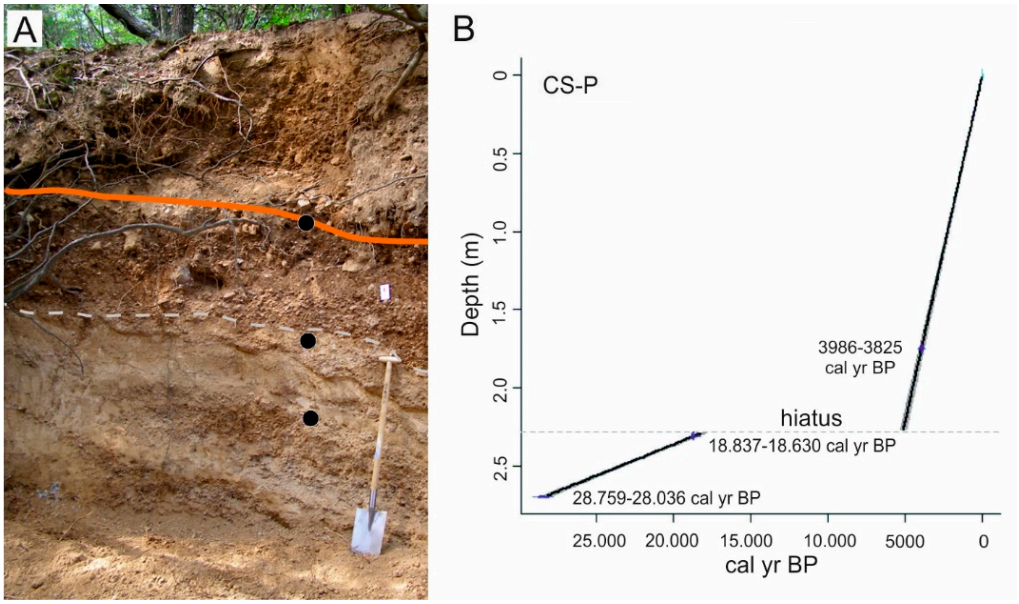

Figure 3. A. Outcrop of CS-P profile in the occasional stream bed in an alluvial fan on the southern shores of Lake Vrana. The orange line represents the identified layer with pottery fragments correlated to this layer in the N-4 profile in the SSW shores of the lake. B. Linear depth-age model, indicating the age of the sediments in the CS-P profile, apparently containing depositional hiatus below the contact between colluvial and loess-like sediments at 2.28 m depth, because of the big age difference between the dates at 1.75 and 2.31 m.

2.3. Laboratory Analyses

In the laboratory, the sediment cores from location VR-1A were split longitudinally in the total length of 7.32 m (+10 cm in core catcher). The interval between 0 m and 4.40 m and 14-cm long base of the core (7.18-7.32 m) was sectioned, both archive and working halves, in 1-cm continuous intervals. The samples from the core catcher were sectioned in 5 cm intervals (7.32-7.37 m and 7.37-7.42 m) Samples from the working half were dried at 40°C in a dryer. The sections between 4.50 m and 7.18 m remained unsampled as the age was undetermined (out of the radiocarbon dating limit), and only color and magnetic susceptibility measurements on the split half were performed. All archived samples and split halves were stored in a refrigerator and cooling chamber for further analysis. Short cores VJ-8 (0.92 m) and VJ-10 (0.74 m) were sectioned at 2-cm intervals in the laboratory and dried for geochemical and mineralogical analysis.

2.3.1. Sedimentological Analyses (Sediment Lightness, Magnetic Susceptibility and Grain Size)

Sediment color of sediment core VR-1A was measured using an X-Rite spectrophotometer in the *L*a*b** values. The magnetic susceptibility (MS) was measured using a Bartington loop (MS2C) sensor at 3-cm intervals, and a point surface (MS2E) sensor at 1-cm intervals, and the values are expressed in SI units ($\times 10^{-5}$) for volumetric low field MS (k_{LF}). This was performed throughout the complete sediment core VR-1A down to 7.32 m. The magnetic susceptibility using Bartington MS2B dual-frequency sensor (mass MS at low frequency – χlf, frequency-dependent MS – χfd) was performed in the sediments from cores VR-1A (46 samples up to 4.40 m and 7.18-7.37 m), CS-5 (5 samples), CS-9 (7 samples) and CS-P (7 samples). Fine-grained samples were packed in 10 cm^3 plastic pots and measured at two frequencies (0.465 and 4.65 kHz). Grain-size analysis was carried out on 97 samples throughout the sediment core VR-1A using a laser diffractometer Shimadzu-SALD 2300. The samples were pre-treated with 30% hydrogen peroxide (H_2O_2) on a hot plate at 80°C to eliminate organic matter, while a dispersant agent ($Na_4P_2O_7$) and ultrasound treatment were used prior to measurement. Data processing for each sample was carried out based on an average of three runs

 doi:10.20944/preprints202408.2193.v1

using the software GRADISTAT v8 [48]. The results were visualized using the C2 software for downcore variations [49].

2.3.2. Mineralogical Analyses

Samples for mineralogical analyses were ground into fine powders using an agate pestle and mortar. Bulk mineralogical analyses were performed using an X'Pert Powder diffractometer (XRD) equipped with a Ni-filter CuKa radiation, a vertical goniometer with θ/θ geometry, and a PIXcel detector. Scan conditions were set at 45 kV and 40 mA, along with ¼ divergence and antiscatter slits, with a step size of 0.02°2θ and a 4 s time per step within a range between 4°2θ and 66°2θ. XRD diffractograms were analyzed using the X'Pert High Score Plus and the ICDD database (PDF-4/Minerals) to determine the qualitative mineral compositions. Detailed clay minerals analysis on oriented glass slides has been applied to selected samples.

Carbonates were removed from the samples prior to mounting the oriented aggregates using buffered sodium acetate (NaOAc) solutions, while the clay fraction (<2 mm) was separated by centrifugation. The samples were then oriented by wet smearing on glass slides to enhance the preferred orientation of clay minerals, thereby increasing the intensity of their basal reflections for identification. A series of diagnostic tests were then applied: air-dried (AD) state, overnight solvation with ethylene-glycol (EG) vapor, and heating to 400°C and 550°C for at least half an hour; treating with dimethyl-sulfoxide (DMSO); heating to 350°C of K-saturated samples; treating with glycerol Mg-saturated samples. Clay samples were then x-rayed after each treatment, across the range between 5° 2θ and 30° 2θ, and individual clay minerals were identified using their basal reflections [50,51]. Chlorite is confirmed by maximums at 14 Å and 7 Å, which remains after treatment with EG and heating, as well as after saturation with K and heating at 350°C. However, after heating of K-saturated sample, if there is an increase in the intensity of the maximum at 10 Å, this means that hydroxy-interstratified vermiculite is also present in the sample. The other maximums of chlorite at 7.1 Å and 3.53 Å coincide with the maximum of kaolinite, which disappears after heating to 550°C. Kaolinite is determined by treatment with DMSO to be well-crystallized (ordered) and poorly-crystallized (disordered), with very clear maximum at 7 Å (disordered) and 11.2 Å (ordered). Illite is determined using maximums at 10 Å and 5 Å, which remain unchanged after all diagnostic procedures. Smectite has a maximum at 14 Å, which after treatment with EG shifts to 17-18 Å, and after heating collapses to 10 Å. However, if part of the maximum at 14 Å remains after EG and after heating, and upon heating the K-saturated sample, chlorite is also present. The K-saturated sample also showed a higher intensity at 13 Å, and after heating, a much higher intensity at 10 Å, indicating the presence of smectite. Saturation with Mg and glycerol confirmed the presence of chlorite (14 Å) and smectite (17-18 Å). Illite-smectite was recognized by a maximum between 10 Å and 14 Å in the AD state, and it shifted towards higher d-spacings when glycolated.

The analysis was performed on 57 powder samples collected throughout the sediment core VR-1A, 15 samples from profile CS-P, four samples from sediment core CS-5, and seven samples from sediment core CS-9. Detailed clay mineral analysis was performed on 13 samples from the sediment core VR-1A and representative samples from CS-P (seven samples), CS-5 (two samples), and CS-9 (two samples). In addition, selected 13 samples from the sediment core VR-1A were semi-quantitatively analyzed using Profex software [52] and Rietveld refinement, which is based on a library of mineral phase structures. Prior to scanning, the samples were mill in a McCrone micronizing mill with ethanol for homogenization to reduce the material to a very fine fraction (<5 μm powder). Mixed-layered clay minerals (illite-smectite) and hydroxy-interstratified vermiculite were not analyzed and presented in semi-quantitative results, as there were no available mineral structures to perform Rietveld fitting.

2.3.3. Geochemical Analyses

Determinations of major, minor, and trace elements were performed on 96 selected discrete powder samples distributed throughout core VR-1A, 15 samples from the CS-P profile, and 50 samples from each of cores CS-5 and CS-9. The samples were treated with near-total hot acid

 doi:10.20944/preprints202408.2193.v1

digestion (HCl-HNO_3-$HClO_4$-HF at 200°C) for these analyses and measured using inductively coupled plasma mass spectrometry (ICP-MS) and inductively coupled plasma atomic emission spectroscopy. The total of 46 elements (Ag, Al, As, Au, Ba, Be, Bi, Ca, Cd, Ce, Co, Cr, Cu, Fe, Hf, In, K, La, Li, Mg, Mn, Mo, Na, Nb, Ni, P, Pb, Rb, Re, S, Sb, Sc, Se, Sn, Sr, Ta, Te, Th, Ti, Tl, U, V, W, Y, Zn, Zr) were analyzed in the Bureau Veritas (Vancouver, Canada; former ACME laboratory), but due to the detection limits and accuracy, only selected elements were used. Elemental compositions were normalized to Al to remove carbonate dilution effects on bulk sediments [53].

Total Carbon (TC), Total Nitrogen (TN), Total Organic carbon (TOC), and Total Inorganic carbon (TIC) were measured using a CN elemental analyzer (Thermo Fisher Flash2000. Total carbon (TC) and nitrogen (TN) were measured directly, whereas total organic carbon (TOC) was measured after the removal of carbonates using 4M HCl and heating for 2 h. The total inorganic carbon (TIC) was calculated as the difference between TC and TOC. The C/N ratio was calculated by dividing TOC and TN. A total of 96 samples from sediment core VR-1A were analyzed.

Software C2 was used to present the results in downcore variations [49], while STATISTICA7 [54] was used for statistical analysis.

2.3.4. Radiocarbon Dating

The ages were established based on the lake sediment core from the central deep part of the lake (VR-1), where five samples were collected. The analyses have been performed in Radiocarbon laboratory, Institute of Physics, Centre for Science and Education, Silesian University of Technology (Gliwice, Poland) and in Beta Analytic Inc. (Miami, USA). For the topmost part of the sediment core, the dates from the short core VJ-8 were applied (taken from 29).

Sediment cores on the southern shores of Lake Vrana have been dated using charcoals in Beta Analytic Ltd. (USA); four dates in the CS-5 sediment core and seven dates in the CS-9 sediment core. The date from the CS-9 333-338 cm interval was excluded from the depth-age analysis as an outlier due to the date inversion from the two following, deeper samples.

The sediment profile on the southern shore of the lake was dated using one date (CS-P 231), while the other two dates were correlated based on the determined sediment sequence. The sediment layer, which contains pottery material, is found in the N-4 profile and also on the southern and southwestern shores of the lake, which could be followed in this CS-P profile. Therefore, this age was applied to layers containing pottery fragments. The age of the lower part of the sequence was determined based on the CS-6 sediment core at interval of 30-35 cm, which is interpreted as a loess-like material. They could correspond to the lower sequence in the CS-P profile, approximated to a depth of 270 cm.

The measured ages (^{14}C BP) were converted into calendar years using the calibration curve IntCal20 Northern Hemisphere [55] using the Clam 2.5 software [56]. Using the same software, the depth-age models using linear interpolation were built for the cores VR-1A, CS-5 and CS-9 (Figure 4) and the profile CS-P (Figure 3). All summarized radiocarbon dates are presented in Table 1.

Table 1. Radiocarbon dating of the analyzed sediments (GdA-Gliwice, Poland laboratory; Beta-no.-Beta Analytic Inc. laboratory; ND-not defined; NA-not analyzed). [1]Data from 29; [2] Original sample names.

Core	Depth (cm)	Lab. no.	Material	$\delta^{13}C$ (‰)	Radiocarbon age (^{14}C BP)	Calendar age (calibrated) - 95% probability (cal yr BP)
VJ-8[1]	18	/	Wood, plant	ND	300 ± 40	470-290
VJ-8[1]	37	/	Wood, plant	ND	500 ± 25	543-506
VR-1A	77-78	GdA-3300	Wood, plant	ND	1870 ± 25	1828-1715
VR-1A	189-190	GdA-3301	Wood, plant	ND	7155 ± 30	8019-7933
VR-1A	317-318	GdA-3302	Wood, plant	ND	10.400 ± 35	12.483-12.092
VR-1A	521-523	Beta-328265	Mollusk	-2.5‰	NA	> 43.500 BP

 doi:10.20944/preprints202408.2193.v1

VR-1A	733-735[1] (725-727 cm)	Beta-328266	Mollusk	-1.2‰	NA	> 43.500 BP
CS-5	106-110	Beta-229818	Charcoal	-25,6	4280 ± 40 BP	4962-4816
CS-5	188-198	Beta-2229819	Charcoal	-25,7	6200 ± 40 BP	7171-6983
CS-5	360-370	Beta-229823	Charcoal	-24,9	6660 ± 50 BP	7607-7461
CS-5	501-506	Beta-229824	Charcoal	-24,6	7360 ± 50 BP	8220-8028
CS-9	42-44	Beta-228408	Charcoal	-23,3	880 ± 40 BP	835-721
CS-9	270-275	Beta-229820	Charcoal	-25,6	5910 ± 50 BP	6858-6632
CS-9	283-288	Beta-229821	Charcoal	-26,2	6130 ± 40 BP	7158-6931
CS-9	303-308	Beta-229822	Charcoal	-24,8	6290 ± 40 BP	7315-7156
CS-9	333-338	Beta-228414	Charcoal	-25,3	7030 ± 40 BP	7944-7777
CS-9	433-438	Beta-228415	Charcoal	-23,3	6530 ± 40 BP	7510-7417
CS-9	515-525	Beta-228416	Charcoal	-23,3	6650 ± 40 BP	7582-7463
N-4 248-259[2]	174-176	Beta-199264	Charcoal	-24.2	3590 ± 40 BP	3986-3825
CS-P 231	231	GdA-3303	Wood, plant	ND	15.390 ± 60	18.837-18.630
CS-6 30-35[2]	270	Beta-228407	Charcoal	-23.3	24.260 ± 120	28.759-28.036

3. Results

3.1. Sedimentation Rates

The age-depth models of the studied cores gave a maximum age of 16.4 cal kyr BP for the VR-1A core at 4.40 m, based on the assumption of a constant sedimentation rate after the last dated interval age of 12.2 cal kyr BP at 317-318 cm. The rest of the core to the base remained undated and was considered to belong to the Late Pleistocene age. The two analyzed samples of freshwater mollusk shells at lower depths (5.21-5.23 m and 7.25-7.27 m) had extremely low ^{14}C activity, almost identical to the background signal, therefore the result is considered greater than the radiocarbon dating limit (Table 1). The dates from short core VJ-8 were incorporated into the depth-age model for the upper part of the core (Figure 4A).

The CS-5 record has a maximum age of 8.2 cal kyr BP at 5.19 m sediment depth while the CS-9 record spans over 7.5 cal kyr BP at 5.51 m depth (Figure 4A). In both cores, a constant sedimentation rate is assumed for the remaining undated part of the core (from 5.03 m to 5.19 m for CS-5 and from 5.20 to 5.51 m for CS-9). The sedimentation rate of the upper parts of the sediment core CS-5 is 0.02 cm/yr and 0.04 cm/yr, from 0-4.8 cal kyr BP and from 4.8-7.0 cal kyr BP, respectively (Figure 4B). At the age between 7.0 and 8.2 cal kyr BP (1.87-5.19 m) in core CS-5, the sedimentation rate increases significantly, to 0.4 cm/yr at 3.65-1.87 m and 0.2 cm/yr at 5.19-3.65 m. The upper parts of the core CS-9 down to 2.85 m (7.0 cal kyr BP) reveal a similar sedimentation rate (0.04 cm/yr) to the upper parts of CS-5. After 2.85 m, it starts to increase to 0.11 cm/yr down to 3.05 m, 0.60 cm/yr to 4.35 m, and 0.85 cm/yr to the base of the core to 7.5 cal kyr BP. The event layer, identified in the CS-5 and CS-9 records, showed similar ages and might represent the same regional event. Erosional events are determined in the core VR-1A at the similar age, with the peak between 4.9 and 8.0 cal kyr BP (1.34-1.90 m) and in the topmost part of the core, in the last 400 years (upper 0.20 m).

The age of the sediment profile CS-P was determined based on the correlation with the two other previously sampled profiles, with the sediment layer containing ceramic material and loess-like material that appeared lower than 2.28 cm (Figure 4). There is a large age difference between the

 doi:10.20944/preprints202408.2193.v1

dates at 1.75 and 2.31 m, therefore it is determined that hiatus in deposition must have occurred below the contact between colluvial and loess-like sediments at 2.28 m depth.

3.2. Sedimentological, Mineralogical and Geochemical Description of Sediment Cores VR-1A, CS-5, CS-9 and Profile CS-P

The VR-1A sediment core is 7.32 m long (+0.10 m of core catcher=7.42 m; 7.32-7.37 m and 7.37-7.42 m). In this study, we robustly included the whole sequence to gain insight into the sediment composition using sediment color (i.e., lightness parameter *L**) and magnetic susceptibility (MS2C in lower and MS2E in higher resolution) throughout the core. The sediment sequence was divided into ten units (Figure 6). The sediments from 4.40 m upwards were analyzed in detail using sedimentological, mineralogical, and geochemical proxies. This was complemented with the sectioned base of the core at interval 7.18-7.37 m.

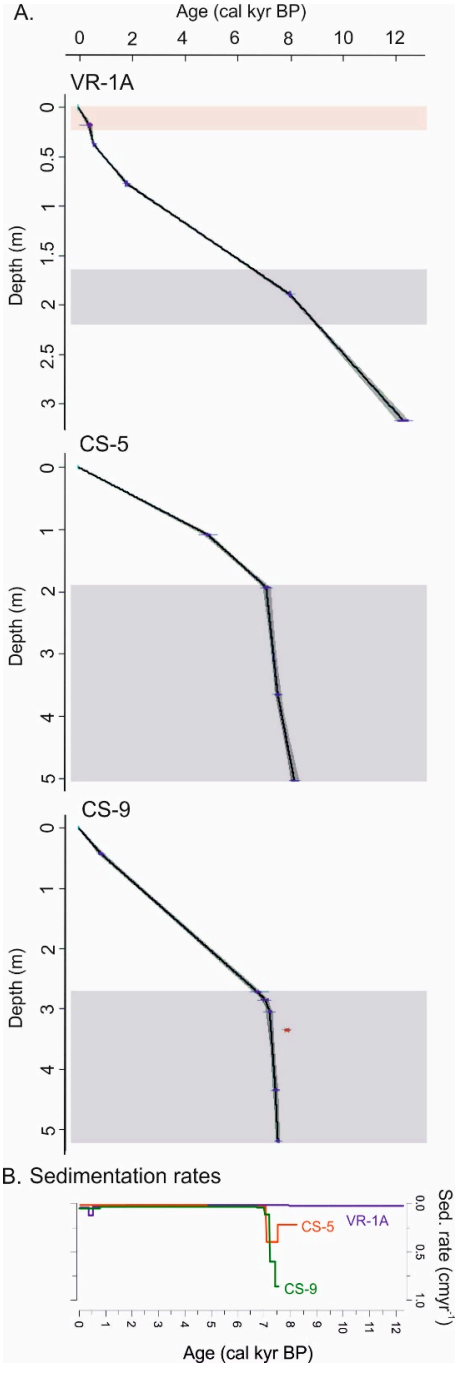

 doi:10.20944/preprints202408.2193.v1

Figure 5. A. Age-depth models of sediment cores from the center of the lake (VR-1A) and on the southern shores of the lake (CS-5 and CS-9). Calibrated 14C ages are shown in blue, while the red age in core CS-9 indicates a reversed date. The horizontal gray-shaded rectangles represent the same erosional event, and the topmost erosion in core VR-a is marked by an orange rectangle. B. Sedimentation rates of analyzed cores.

From the base of the core (7.37 m) up to 6.50 m, the sediments are darker, brown in color, quite solid, and compact, with a slightly higher magnetic susceptibility than the following upper section (Figure 6). There is an evident peak in the magnetic susceptibility at 7.03-7.05 m (MS2E ~20 $\times 10^{-5}$ SI). From 6.50 m, there is a transition to brighter sediments which spans up to 3.80 m with similar values of magnetic susceptibility (except one more peak at 4.00 m; MS2E 13 $\times 10^{-5}$ SI). The median value of magnetic susceptibility (MS2E) between 6.5 m and 3.80 m is 4.4 $\times 10^{-5}$ SI. At 3.80 m there is a sharp slantwise border with a transition to evidently darker sediment (lower values of lightness parameter L^*), which could indicate lower carbonate content and more organic matter content in sediments [57]. There is also a shift to lower values in magnetic susceptibility in this „dark" zone between 3.80 m and 3.00 m. It is „interrupted" by brighter sediments between 3.30 m and 3.45 m, which appear as lenses mixed with darker sediments. In the next unit between 3.00 m and 2.50 m, there is a trend of increasing magnetic susceptibility values. Sediments are relatively dark, but in the interval between 2.50 m and 2.70 m there are almost completely black layers that appear as laminae of various thicknesses: at 2.53 m 10 mm thick, at 2.56 m 3 mm thick, at 2.58 m 3 mm thick, at 2.59 m 1 mm thick, at 2.60 2 mm thick, black layer at 2.65-2.70 m with very thin lenses of brighter sediments. From 2.50 m up to 1.25 m, the magnetic susceptibility values are the highest, with the peaks between 1.90-1.65 m and 1.50-1.34 m, where the median values are 14.4 $\times 10^{-5}$ SI. From 1.25 m to 0.70 m there was a decrease in magnetic susceptibility values, and the sediments were dark in color. Moreover, black layers are present in almost the entire interval, at 1.09-1.02 m, 0.98-0.95 m and 0.79-0.73 m. An increase in sediment lightness is apparent from 0.70 m up to 0.20 m and magnetic susceptibility is relatively low. In the sediment from 0.20 m up to the top-most sediments, magnetic susceptibility increases and sediments are darker in color.

The upper 4.40 m of the sediment core VR-1A (which is dated) was interpreted using dual-frequency magnetic susceptibility (MS2B), grain size, mineralogical (XRD), and geochemical analyses (Supplementary Materials S1) to determine variations in carbonate and siliciclastic material, as well as inorganic and organic carbon content (Figure 7).

The first zone 4.40-3.80 cm (16.4-14.4 cal kyr BP) is the continuation of a previously robustly determined unit based only on sediment lightness and magnetic susceptibility (from 6.5 m, undated). The sediments are determined as carbonate, bright gray sediments, and dominantly coarse silts, with median silt values of ~80%. In addition, one clast, 0.5 1 cm diameter) was noticed at 3.89 m, which indicates high water energy. The sediments are characterized by low mass magnetic susceptibility (median ~5 $\times 10^{-8}$ m^3/kg) and siliciclastic content (Al, quartz, muscovite/illite, clay minerals), whereas the carbonate content is higher (Ca, calcite, dolomite). Smectite, chlorite, illite, and kaolinite were present in the clay mineral fraction. The carbonate content was also indicated by a higher total inorganic carbon (TIC) content. This is similar to the grain-size composition of the undated base of the core (7.37-7.18 m), which are also coarse silts but contain predominantly dolomite as a mineral phase, with minor phases of calcite, quartz, muscovite/illite, plagioclase, and clay minerals. The sediments from the base of the core differ from those from the upper unit in clay mineral composition and contain chlorite, hydroxy-interlayered vermiculite, illite, and kaolinite. In the sediments at the base of the core, the total organic carbon (TOC) had a value of 1.2%, while in the overlying sediments from the zone 4.40-3.80 m TOC is 0.4%.

 doi:10.20944/preprints202408.2193.v1

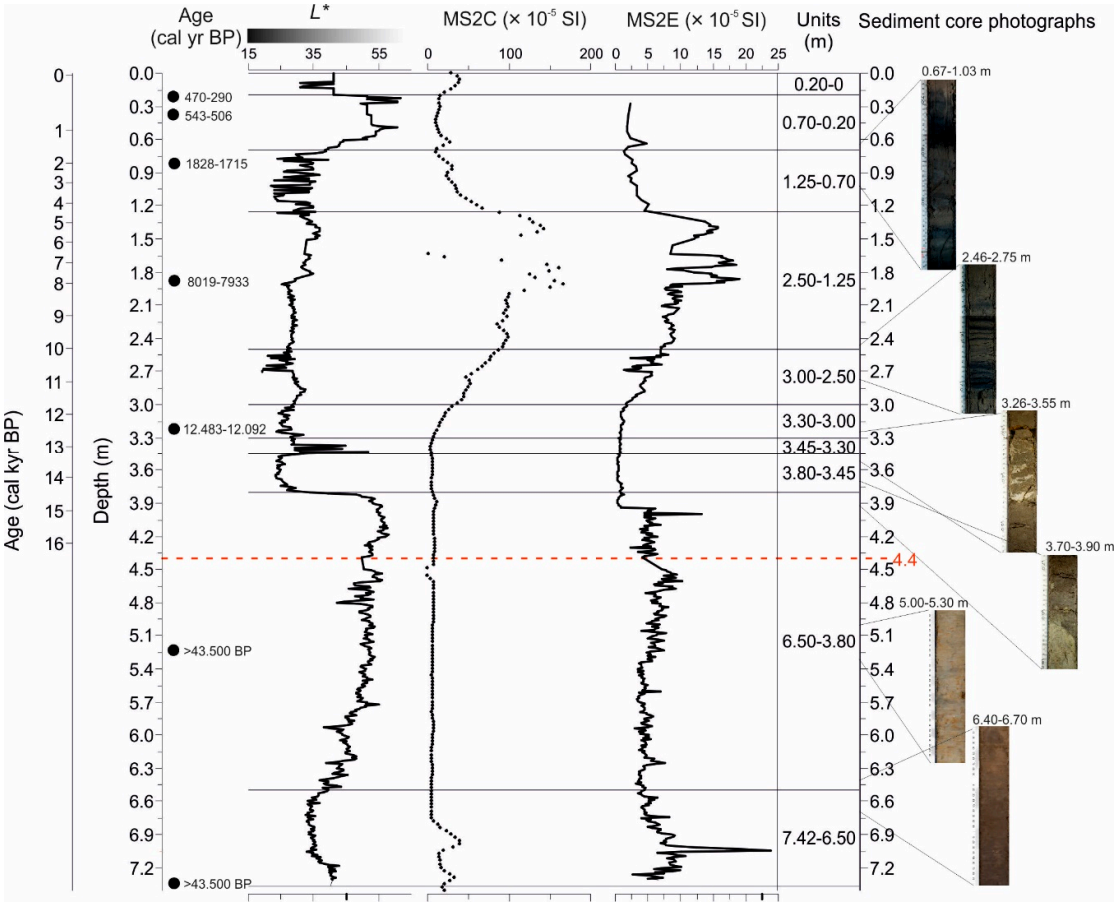

Figure 6. Sediment lightness (*L**) and magnetic susceptibility (MS2C and MS2E; k_{LF}) throughout the complete sediment core VR-1A 0-7.37 m, with indicated dated intervals and ages as well as identified units. Selected sediment photographs are also shown. The red dashed line at 4.4 m represents the upper section of the core analyzed in detail.

The total organic carbon (TOC) content increased up to 6.9% in zone 2 (14.4-13.3 cal kyr BP, 3.80-3.45 m). The remains of the plant material and gastropods appear sporadically. The sand fraction increases up to 46.8% and these sediments are very coarse to coarse silts. The major mineral phase is quartz, with minor dolomite, plagioclase, muscovite/illite and clay minerals (smectite, chlorite, illite and kaolinite), which is evident in higher siliciclastic contents (Al, Ti, Fe, K, Na). There is a sharp change in sediment deposition in the next zone 3, 13.3-12.7 cal kyr BP, in the interval between 3.45 m and 3.30 m, evident in lower sand fraction (18.3-30.8%), TOC (0.6-5.1%) and siliciclastic content (Al, quartz, muscovite/illite) and with increased carbonate content (Ca, Sr, calcite, dolomite, aragonite). There were apparent plant remains and visible seeds, as well as small gastropod shells.

In the following zone 4, 12.7-11.7 cal kyr BP (3.30-3.0 m), siliciclastic content increases (Al, Ti, Fe, K, but lower Na), and quartz, muscovite/illite, and clay minerals are present, with less dolomite. The TOC content and sand fraction were high (4.4-7.8% and 26-35.8%, respectively), similar to zone 3. The remains of plant materials are visible in the sediment.

 doi:10.20944/preprints202408.2193.v1

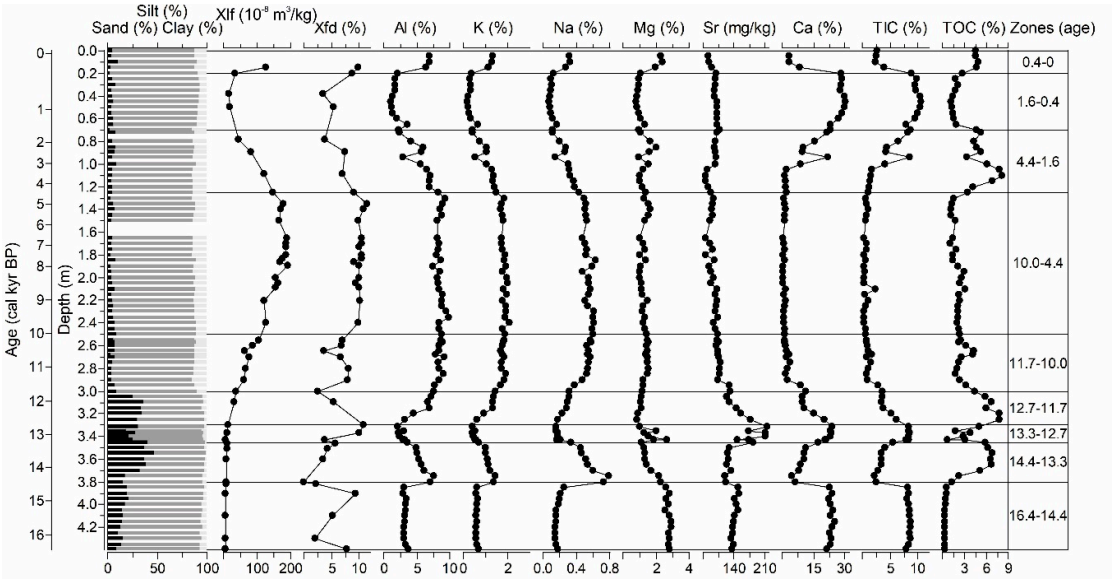

Figure 7. Downcore variation in core VR-1A (0-4.4 m) grain size, mass magnetic susceptibility (χlf), frequency-dependent MS (χfd), and selected geochemical elements (Al, K, Na, Mg, Sr, Ca, TIC, TOC), with zones identified by age (cal kyr BP).

An increasing trend in magnetic susceptibility parameters (mass and frequency-dependent MS) is visible in zone 5 between 11.7-10.0 cal kyr BP (3.00-2.50 m) as well as in Al, dolomite, quartz, feldspar, muscovite/illite, and clay mineral content. Here, we observe a change in the clay mineral assemblage, similar to the base of the core, which is determined as chlorite, hydroxy-interlayered vermiculite, illite, and kaolinite. These clay minerals remained in the sediments in the entire upper section from here to the top. Sediments are finer from this unit upward to the top (3.00-0 m) and are interpreted mainly as medium to fine silts, with median values of sand, silt, and clay fractions of 5.4%, 81.7%, and 12.3%, respectively. TOC values are decreasing in zone 5, although there is an increase in TOC content to ~4% in the interval 2.70-2.50 m (10.7-10.0 cal kyr BP), where black laminations of various thicknesses appear.

In zone 6, 10.0-4.4 cal yr BP (2.50-1.25 m), magnetic susceptibility further increases, with maximum values (median mass MS ~180 $\times 10^{-8}$ m^3/kg) in the interval between 1.90 m and 1.34 m (8.0 cal kyr BP and 4.9 cal kyr BP). Siliciclastic component (represented by Al content) is also increased in this unit, with quartz as the dominant mineral phase, while calcite is absent and only small proportions of dolomite sporadically appear, as well as amphibole. Carbonate elements (Ca, TIC) are constantly low. TOC content is slightly elevated (med. 2.4%) from 10.0-8.0 cal kyr BP (2.00-1.90 m), while lower values (med. 1.4%) are recorded from 8.0-4.4 cal kyr BP (1.90-1.25 m).

In zone 7, 4.4-1.6 cal kyr BP (1.25-0.70 m), TOC content increases from 3.4% to 8.2%. Compared to the previous unit, the magnetic susceptibility parameters and Al content decreased. From 0.94 m upwards, the content of Ca and TIC values is increasing. In this zone, sediments are mainly composed of quartz, with minor dolomite and muscovite/illite, and accessory calcite, whereas calcite appears in higher amounts in the upper part of the unit.

This continues to zone 8, 1.6-0.4 cal kyr BP (0.70-0.20 m), with increased carbonate content evident in higher Ca and TIC values, and calcite as the dominant mineral phase (quartz and dolomite are minor components). TOC values decreased to relatively low values (1.2-2.1%) compared to the lower zone and increased in the upper 0.20 m of the sediment core, where the TOC median was 4.6%.

In zone 9 (0.4 cal kyr BP, 0.20 m), the carbonate content (Ca, TIC, calcite) is lower, while magnetic susceptibility and siliciclastic components (Al, quartz, muscovite/illite), as well as dolomite, are higher. The semi-quantitative mineralogical composition (in wt%) revealed the above-mentioned variations in the mineralogical composition (Figure 8).

 doi:10.20944/preprints202408.2193.v1

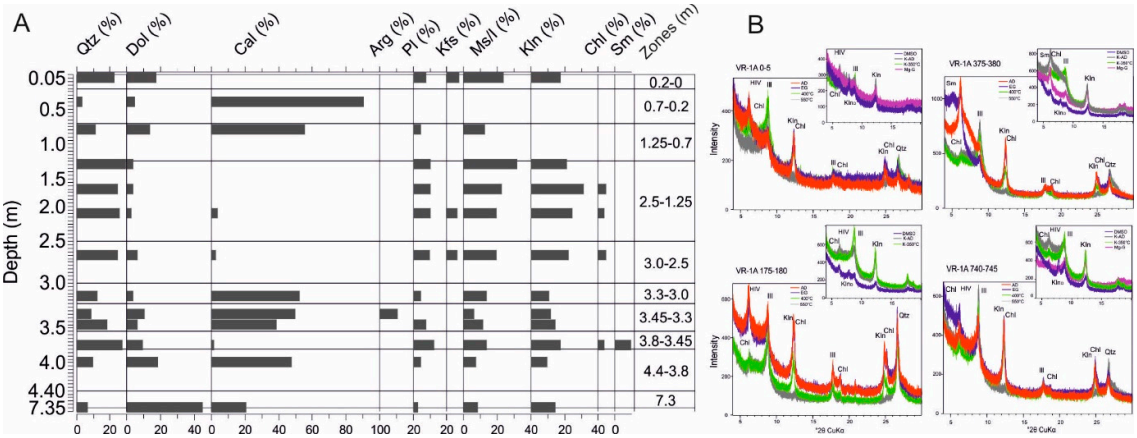

Figure 8. A. Semi-quantitative mineralogical composition of the sediment core VR-1A, with sedimentary units shown on the right (in m). B. XRD patterns of selected samples for different diagnostic tests for clay mineral composition. Abbreviations: Qtz-quartz, Dol-dolomite, Cal-calcite, Pl-plagioclase, Arg-aragonite, Kfs-alkali feldspar, Ms/I-muscovite/illite, Kln-kaolinite, Chl-chlorite, Sm-smectite, HIV-hydroxy interlayered vermiculite.

The geochemical compositions of the short sediment cores VJ-8 and VJ-10 (Figure 9) were used to complete the lake-sediment interface in the sediment core VR-1A using the dated material from VJ-8 [29]. In the short core VJ-8, a low siliciclastic content (Al) and high Ca content in the lower part of the core (0.86-0.43 m) could be correlated to the interval 0.70-0.20 m in cores VR-1A and VJ-10. The dominant mineral phase is calcite, while the minor is dolomite, quartz, and muscovite/illite. In all three cores, next zone is marked by increasing Al concentration and decreasing Ca content, which lasts in core VJ-8 up to the 0.08 m, while in core VJ-10 up to the 0.04 m. In this siliciclastic phase, the samples from cores VJ-8 and VJ-10 appear predominantly quartz and dolomite with minor calcite. Core VR-1A ended with an elevated Al content in the surface sample. In the core VJ-8 Ca content increases after 0.08 cm, and in core VJ-10 after 0.04 m, and this marks the re-establishment of carbonate sedimentation in the last 100 years (-50 od 1950). This interval was added as zone 10 in the VR-1A sediment core paleoenvironmental reconstruction. The sediments contained more calcite, dolomite, quartz, and clay minerals. In clay mineral fraction, throughout the core VJ-8, chlorite illite, and kaolinite are present in the clay mineral fraction, with the possible presence of hydroxy interlayered vermiculite.

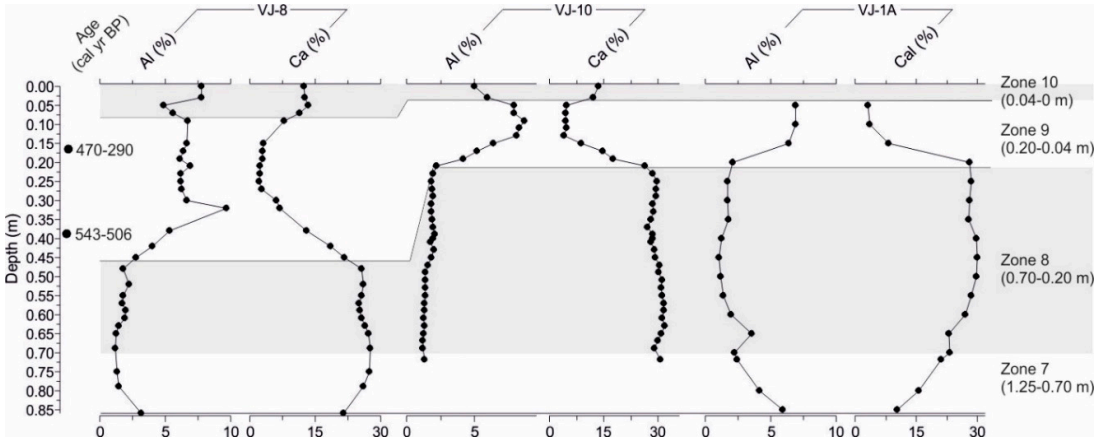

Figure 9. Geochemical records (Al, Ca) of the short cores VJ-8 and VJ-10, compared to VJ-1A, for the undisturbed topmost sediment sequence (<0.86 m). Age was determined using core VJ-8. The grey background in all cores marks the carbonate zones, lower and uppermost, recorded in the sediments.

 doi:10.20944/preprints202408.2193.v1

In the sediment core CS-5, which along its entire length of 5.19 m represents lithologically red soils (terra rossas), three sedimentary units were distinguished according to geochemical and mineralogical composition (Figure 9). These changes were based on the variable proportions of Al and Ca as representatives of the deposition of siliciclastic and carbonate materials. In the deepest part of the core, from 5.19 m to 1.87 m, which corresponds to the period between 8.2 and 7.0 cal kyr BP, there is a relatively high concentration of Al, as well as other lithogenic elements (Ti, Fe, K, Na), and low concentrations of Ca and Mg. This relatively short time period of only 1200 years is characterized by high sedimentation rates (median 0.4 cm/yr), and more than 3 m of siliciclastic sediments were deposited. Mineralogically, the dominant phase was quartz, with minor muscovite/illite, feldspar, dolomite, amphibole, and clay minerals. Chlorite, hydroxy-interlayered vermiculite, illite, and kaolinite appear in the clay mineral composition, which remains the same in the upper sections of the CS-5 core. The mass magnetic susceptibility (χlf) was high in the CS-5 core and ranged between 132 and 202 ×10-8 m^3/kg. The percentage of frequency-dependent MS (χfd) ranged between 8.5% and 10.8%. From 6.9-2.4 cal kyr BP (1.87 m to 0.54 m), the Al content gradually decreases, which is also visible in the mineralogical composition, where quartz is less abundant but still a major phase, while dolomite peaks show higher intensity with increasing concentrations of Ca and Mg. In the upper unit, 0.54-0 m and the last 2.4 cal kyr BP, dolomite was the main mineral phase, Ca and Mg were higher, while Al content and quartz were significantly lower compared to the previous unit.

The lowest unit of the core CS-9 (5.51-3.47 m) corresponds to the short period between 7.5 and 7.3 cal kyr BP, with the highest sedimentation rate throughout the core (median 0.85 cm/yr). It has elevated siliciclastic elements (Al, Ti, and Fe), and its major mineral phase is quartz, with minor dolomite, muscovite/illite, feldspar, calcite, amphibole, and clay minerals (chlorite, hydroxy-interlayered vermiculite, illite, and kaolinite) (Figure 10). The mass magnetic susceptibility (χlf) is the highest in the core in this unit (71.5-91.4 ×10-8 m3/kg) and is lower in the rest of the core, while the percentage of frequency-dependent MS (χfd) is between 4% and 6%. Similar values were present only in the topmost unit. In the interval 7.3-3.3 cal kyr BP (3.47-1.40 m), Al and Fe contents were lower, while Ca and Mg increased, which was followed by higher amounts of dolomite and calcite. Carbonate elements (Ca and Mg) rapidly increase in the next unit, 3.3-1.7 cal kyr BP (1.40-0.80 m). In the uppermost unit (1.0-0 cal kyr BP, 0.53-0 m), dolomite, calcite and quartz are the main mineral components, while the interval between these two units is marked by the higher siliciclastic elements (Al, Fe), which appeared at 1.7-1.0 cal kyr BP (0.80-0.53 m).

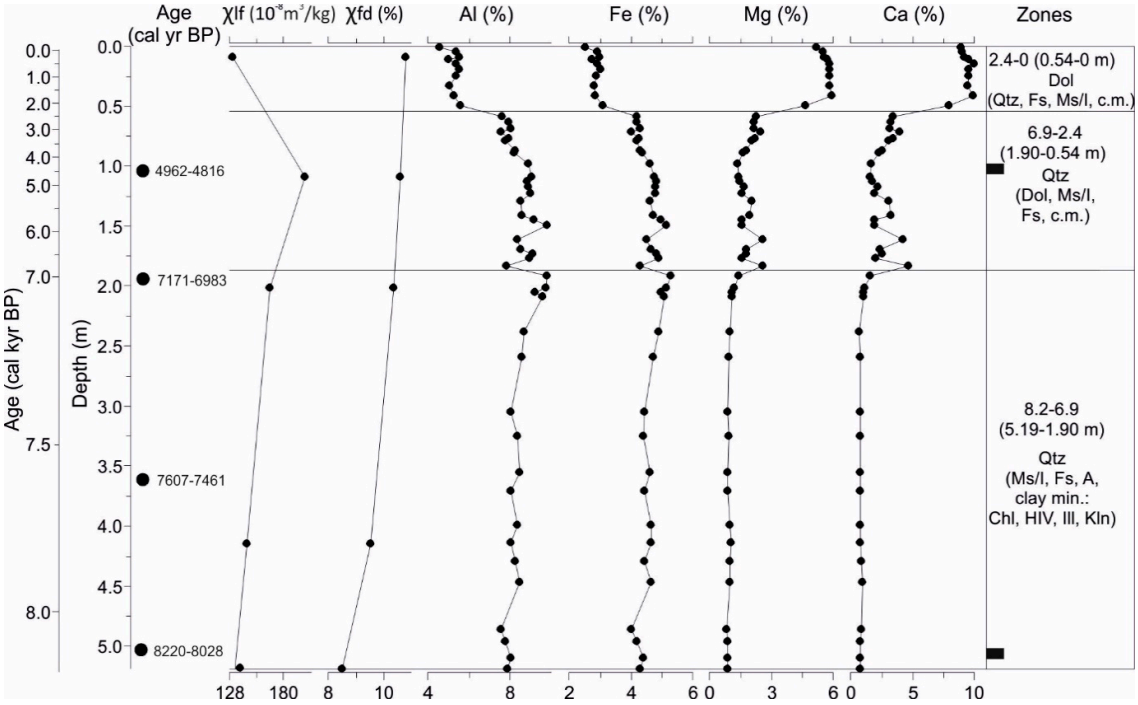

 doi:10.20944/preprints202408.2193.v1

Figure 10. Magnetic susceptibility parameters (χlf, χfd) and selected geochemical elements down-core variations in the sediment core CS-5, with dated samples on the left and zones on the right (in age and depth). The mineralogical composition is shown within these zones. The black rectangles represent the samples analyzed for clay minerals. Abbreviations: c.m.-clay minerals, Qtz-quartz, Dol-dolomite, Fs-feldspar, Ms/Ill-muscovite/illite, A-amphibole, Chl-chlorite, HIV-hydroxy interlayered vermiculite, Ill-illite, Kln-kaolinite.

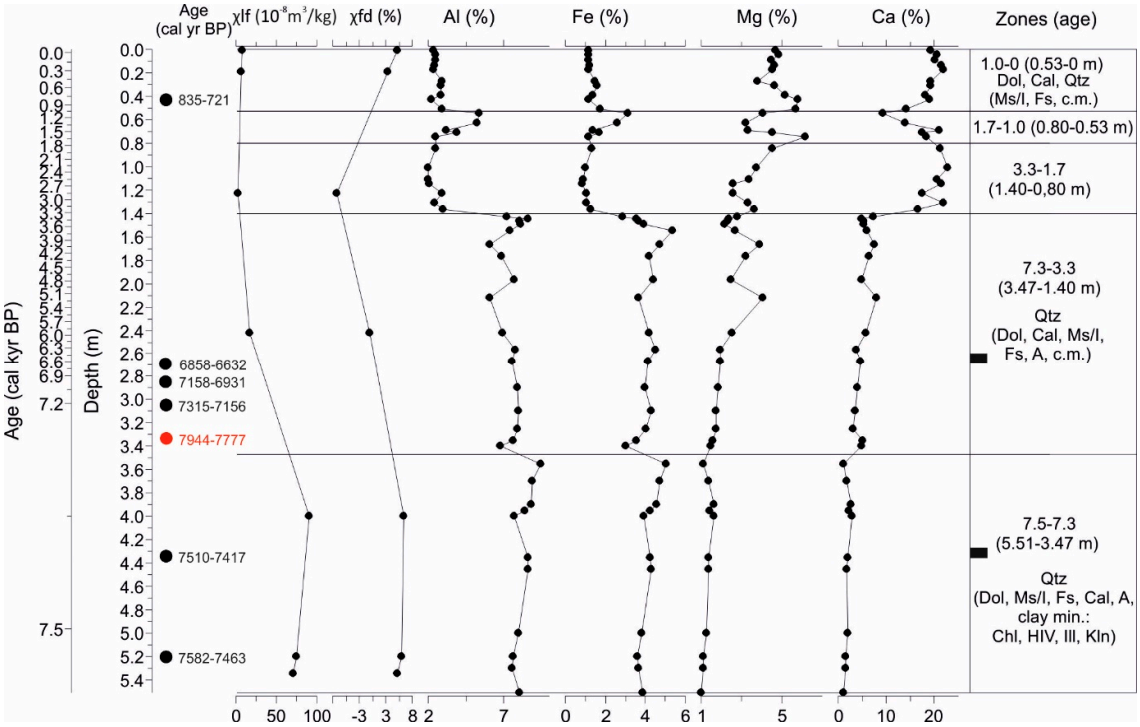

Figure 11. Magnetic susceptibility parameters (χlf, χfd) and selected geochemical elements down-core variations in the sediment core CS-9, with dated samples on the left and zones on the right (in age and depth). The age marked in red was rejected as the reversed date. The mineralogical composition is shown within these zones. The black rectangles represent the samples analyzed for clay minerals. Abbreviations: c.m.-clay minerals, Qtz-quartz, Dol-dolomite, Cal-calcite, Ms/Ill-muscovite/illite, A-amphibole, Fs-feldspar, Chl-chlorite, HIV-hydroxy interlayered vermiculite, Ill-illite, Kln-kaolinite.

Sediment profile CS-P contains loess-like sediments from 3.40 m up to 2.28 m, with an age of 18.7 and 28.4 cal kyr BP, which correspond to the LGM period. There is significant carbonate content in the sediment (higher Ca and Mg), which contains dolomite as a major component, while calcite and quartz appear as minor minerals with variable content. Feldspar was also present throughout the profile, while amphibole was present in the lower section. In the clay mineral composition, chlorite, smectite, illite, and kaolinite appear in the lower section of the loess-like unit, whereas mixed-layer illite-smectite, illite, and kaolinite are present in the upper section. In the colluvial sediment, from 2.28 m upwards, quartz and dolomite appear in similar proportions, with clay minerals including chlorite, hydroxy-interlayered vermiculite, illite, and kaolinite. Dolomite is the dominant mineral phase in the upper 1 m of the profile, with minor quartz, muscovite/illite, feldspar, and clay minerals such as chlorite, illite, and kaolinite.

 doi:10.20944/preprints202408.2193.v1

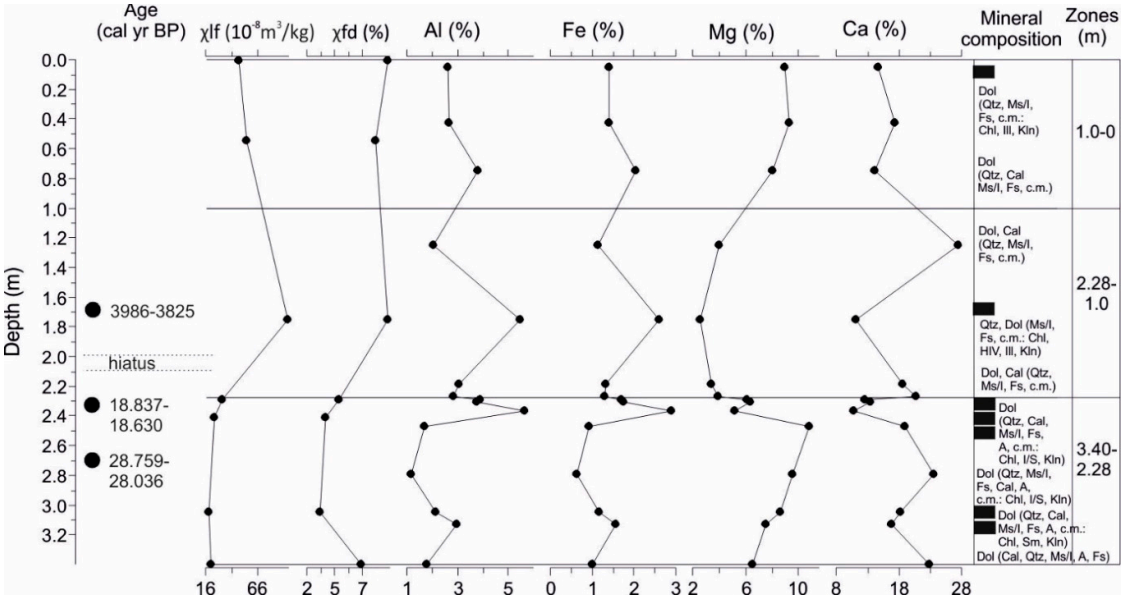

Figure 12. Magnetic susceptibility parameters (χlf, χfd) and selected geochemical elements down-core variations in the profile CS-P, with dated samples on the left and zones on the right (in depth). The mineralogical composition is shown within these zones. The black rectangles represent the samples analyzed for clay minerals. Abbreviations: c.m.-clay minerals, Qtz-quartz, Dol-dolomite, Cal-calcite, Ms/Ill-muscovite/illite, A-amphibole, Fs-feldspar, Chl-chlorite, Sm-smectite, I/S-illite/smectite, HIV-hydroxy interlayered vermiculite, Ill-illite, Kln-kaolinite.

4. Discussion

4.1. Environmental Interpretation of Geochemical and Mineralogical Data and Paleoenvironmental Reconstruction

In general, environmental records of closed lakes such as Lake Vrana carry a signature of past variations in the regional hydrological balance, and the lake level mirrors the depositional conditions. Evidence of lake-level changes in Lake Vrana has been documented by multi-proxy approach studies (cladocerans, diatoms, geochemistry, plant macrofossils, pollen) on sediment cores and seismic acoustic-echosounding profiles [7]. As a limitation of this study, the insufficiently accurately determined age of the sediments using ^{14}C-datable organic material was highlighted [7]; therefore, precise chronological stratigraphy could not be applied. Additionally, an attempt has been made to reconstruct paleolake fluctuations over the last ~2200 years using a lake sediment core close to the lake's northern shore [9].

The paleoenvironmental reconstruction of the evolution of Lake Vrana was based on sedimentological, geochemical and mineralogical analyses of a 7.4 m long sediment core VR-1A, which contains continuously deposited lake sediments without the evidence of a soil environment or paleosol formation that would imply the development of a karst polje. The depositional events, sediment delivery, and lake dynamics were supported by the analyses of the sediment cores and outcrop profiles (CS-5, CS-9, and CS-P) from the alluvial fan in the southern part of the lake.

4.1.1. Late Pleistocene (Base of the Core VR-1A: 7.37-7.18 m)

Lake Vrana on the island of Cres is considered to be of Late Pleistocene age, developed as a karstic depression filled with more than 25 m of lake sediments [7]. The sediments from the analyzed interval 7.37-7.18 m at the base of the core are lithologically described as dolomitic carbonate sediments, with low siliciclastic content, although the magnetic susceptibility is relatively high. This could be attributed to high dolomite content and the presence of clay minerals, and low calcite content. Chlorite, hydroxy-interlayered vermiculite, illite, and kaolinite were present in the clay

 doi:10.20944/preprints202408.2193.v1

mineral fraction. The magnetic susceptibility of sediments is primarily influenced by the concentration of ferrimagnetic minerals, and also related to sediment composition, magnetic mineralogy and grain size [58]. Calcite and quartz are diamagnetic minerals, compared to dolomite and clay minerals, which show higher magnetic susceptibility values due to the paramagnetic contribution [58]. Therefore, it is reasonably assumed that the magnetic susceptibility record from Lake Vrana sediments reflects mineralogical changes. Clay minerals, quartz, and dolomite, and possibly partly calcite, are detrital and derived from the lake catchment.

The lake sediments from the base of the core at 7.42 m up to 3.17 m remained undated due to the only two sampled dates (and a limited source of material for dating) that showing the age out of the range of radiocarbon dating. Therefore, the sediments from the interval from 7.4 to 4.4 m is proposed to be older than 40 cal kyr.

The seismic acoustic profiles from that depth in Lake Vrana [7] were compared with the lacustrine phase detected in seismic units from the Lošinj Channel, which is located between islands Cres and Lošinj [16,17]. These reflector configurations showed similar characteristics, implying a similar environment and age. The Lošinj Channel is only 16 km away from Lake Vrana and holds the record of the MIS 3 (46.5-44.7 cal kyr BP) lacustrine phase (Lošinj paleolake) [16]. This was possible due to the existence of a karstified sill at 50 m b.s.l. in the direction of Kvarnerić Bay. The sill depth determined the isolation of the Lošinj basin with formation of a paleolake or karst polje during the glacial lowstand conditions (MIS 2-4 and MIS 6), whereas during interglacial periods (Holocene and MIS 5), the basin was connected to the sea [16,17]. In contrast to Lake Vrana, Lošinj Channel had karst polje phases during MIS 4 (>46.5 cal kyr BP) and MIS 3/MIS 2 (44.7-13.7 cal kyr BP). During the post-LGM transgression, the marine lake in Lošinj Channel was connected to the sea via karstified underground until Holocene marine transgression and seawater flooding at 10.5 cal kyr BP [16]. Valun Bay, north of Lake Vrana (3 km away), sediments exhibit a Late Pleistocene transition from the late glacial lake phase to the submerged marine bay during the Early Holocene transgression [15]. Similar development of coastal karst basin due to the sea-level rise and the presence of permeable karst, is documented in submerged sinkholes, marine Lake Veliko jezero and Stupa Bay on the island of Mljet [21–23], with terrestrial sediments, i.e. soils, deposited in the basal parts of sediment sequence, during Late glacial, followed by wetland (marsh), shallow lake at 10.8 cal kyr BP, and deep brackish lake and finally ended as a marine lake by sea flooding through the Soline channel (2.5 m deep) at 2.3 cal ka BP.

Therefore, sea level rise had a strong influence on the development and evolution of isolation basins with sills during the Holocene transgression [15–17,21–23]. Such a strong connection to the sea is not evident in Lake Vrana evolution. As a coastal lake only 3–6 km away from the sea on each side, it was assumed that the post-LGM transgression led to the formation of the lake [2,3]. The sea-level curve from MIS 5 to the present is shown in Figure 14A, while the lake development is presented from 14 kyr BP, 10 kyr BP to the present day (Figure 14B-D).

The lake existed as a shallow lake during the proposed MIS-3 age of the recovered sediments at a depth of 7 m, generally constrained between 60 and 29 kyr BP [32], but we do not exclude older ages. Pollen record (form *Buxus*) from the 5 m depth in the sediment core from Lake Vrana indicated that sediments probably originated from interglacial lake deposits [7]. According to [7], the post-LGM rise in sea level was the main reason for an increasing lake level during the wet period, assuming that the sea reduced losses through the karst by forming a local barrier for groundwater, which could be the case. In the total lake sediment infill in Lake Vrana, which is determined to be at least 25 m [7], the age could extend to MIS 5 (127.5-71 kyr BP), the well-known highstand, when the sea level was similar to the present-day level [32]. We believe that the geology of the island of Cres was responsible for the lake water retention in Lake Vrana for longer periods, even during the Late Pleistocene lowstands during glacial periods. Lake Vrana surroundings and catchment are dominated by dolomite rocks [36], which also lie beneath the lake sediments. Dolomites are low-permeability rocks, which could have prevented or significantly slowed down water discharge towards the Adriatic Sea [2]. During the LGM lowstand, the sea was 120-130 m lower than today [30–32,59] and the vast area of the northern Adriatic Sea was dry [16,60–62]. Dolomite rocks govern the hydrology of Lake Vrana

 doi:10.20944/preprints202408.2193.v1

to a great extent both in the past and today. In the past, freshwater is maintained from discharge, and today, prevents seawater intrusion, which was common in Croatian coastal lakes and karst poljes from the Holocene period to the present; Lake Vrana near Biograd [10,11], Velo Blato [12], Bokanjačko Blato [14], Lake Baćina [63].

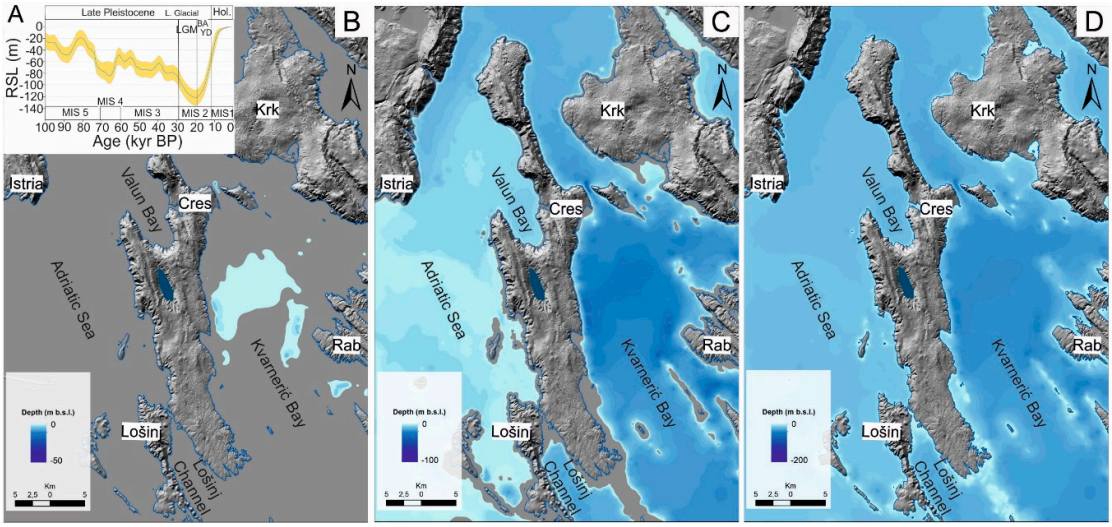

Figure 13. Maps of the sea-level rise during the late Glacial and Holocene and the position of Lake Vrana on the Island of Cres in the northern Adriatic Sea on the eastern Adriatic coast. A. The sea-level curve for the last 100 kyrs (modified from [30]. B. The sea level was ~90 m lower than today, at approximately 14 kyrs ago. C. The sea level was ~40 m lower than today, at approximately 10 kyrs ago. D. Present sea level and coastline.

4.1.2. Late Glacial to Holocene Transition (16.4-11.7 cal kyr BP; Zones 1 to 4)

The maximum age of the studied core VR-1A is 16.4 cal kyr BP at 4.40 m, assuming a constant sedimentation rate after the last dated interval age at 317-318 cm (12.2 cal kyr BP).

The period between 16.4 and 14.4 cal kyr BP (4.40-3.80 m) is characterized by carbonate sediments with dolomite, similar to sediments from the base of the core, but with lower dolomite content. The only possible source of dolomite is detrital, as input from the catchment indicates slightly reduced detrital input by erosion from the surroundings in this period compared to the oldest sediments from the base of the core. This difference is highlighted by the clay mineral composition, which is presented here as smectite, chlorite, illite, and kaolinite. These clay minerals appear in the entire zone up to 11.7 cal kyr BP and point out to a similar sediment source for the whole interval, although with variable carbonate and siliciclastic content. This could correspond to the composition of the loess-like material deposited after the LGM in the lower section of the sediment sequence in profile CS-P, where the hiatus was determined. This means that this material is not preserved in the profile and could be washed away into the lake. A relatively low TOC indicates a cold period, as evidenced by the correlation with the temperature from the Adriatic Sea (Sea Surface Temperature, SST for April–May) [64] and the GISP2 ice core record [65] (Figure 14). The seal level at 14 kyr BP was 90 m lower than today, but the lake existed during this period. The sea emerged only into the Kvarnerić Bay, while the marine lake in Lošinj Channel was formed with marine influence occurring through karstified underground [16] (Figure 14B).

In the period 14.4-13.3 cal kyr BP (3.80-3.45 m), there was a shift to a dominant siliciclastic component in the sediments, with low carbonate content and the highest TOC. This could correspond to erosional events, which were also evident in higher sand fractions and C/N values close to 11, indicating the source of mixed terrestrial and aquatic organic matter [66]. This indicates enhanced sediment discharge through streams and flash flood events into the lake. This could correspond to the Bølling-Allerød (BA) warm and wet period [67], which continues into the next zone.

 doi:10.20944/preprints202408.2193.v1

In the period 13.3-12.7 cal kyr BP (3.45-3.30 m) there is an increase in carbonate content (Ca, TIC and calcite, aragonite), and a simultaneous decrease in TOC values, but C/N ratio remains high. Littoral freshwater gastropod fragments are preserved within this zone. This sediment could be transported through the turbidite currents from the shallow part of the lake. Usually, lacustrine turbidites are associated with earthquakes and seismic activity, as evidenced in Swiss Alpine lakes [68,69]. However, they can also be triggered by other processes like storms and floods. Presumably, this turbidite event must be related to the remobilization of previously deposited subaqueous sediments, which could be the result of Bølling–Allerød warm and wet period.

TOC values increase again, as well as siliciclastic and sand content in the period between 12.7-11.7 cal kyr BP (3.30-3.00 m), followed by decreasing Ca and TIC. This corresponds to the Younger Dryas cold period when general aridity and overall reduced precipitation occurred [71]. In contrast, decreased temperature and vegetation cover can promote soil erosion in catchments and high organic carbon from terrestrial plants [70]. The C/N values higher than 10 indicate the input of terrestrial organic matter washed in from the surrounding catchment, corresponding to mixed phytoplankton and terrestrial sources [66].

In sediments deposited between 14.4-13.3 cal kyr BP, the concentrations of Na normalized to Al values (Figure 14) were high compared to the siliciclastic material in the next zone (12.7-11.7 cal kyr BP), as well as in comparison to the Holocene sediments. This indicates that the deposited material was influenced by the other source material with higher Na content. The source could be magmatic rocks (mainly andesites) in the area of Senjska vrata in Velebit Mt. [72]. These results could suggest a local increase of wind activity, with especially strong bora winds that occur in the area, as a transport mechanism of this material to the lake. These sediments are also more fine-grained (clayey) than older and younger sediments, indicating an eolian origin for this enhanced detrital supply.

This entire sediment sequence (5.00-3.25 m) was interpreted by [7] as sediment erosion and slumping event sediments, which indicated fluctuating lake levels, erosion, and redeposition in a relatively shallow freshwater lake.

 doi:10.20944/preprints202408.2193.v1

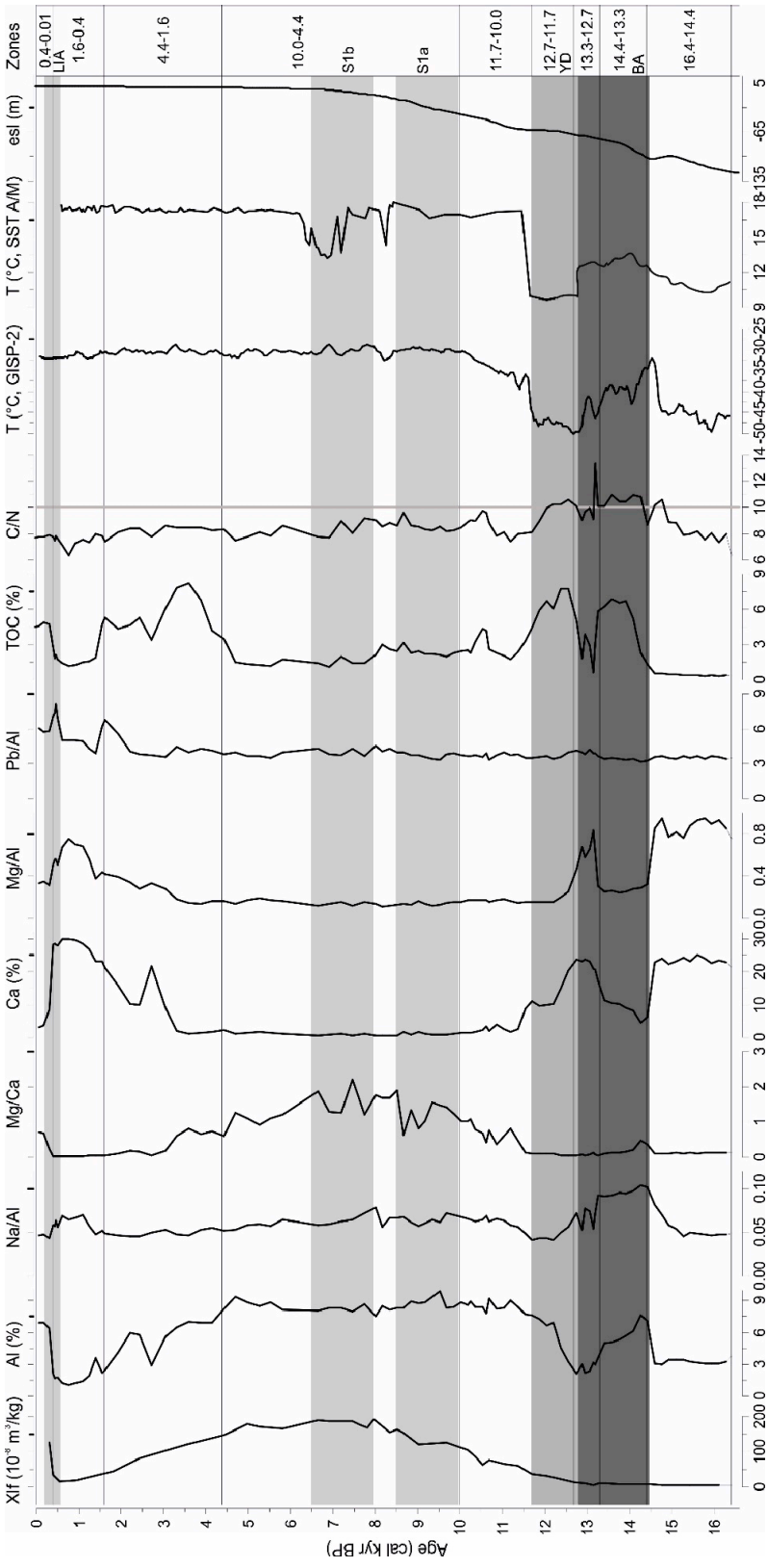

Figure 14. Variation in geochemical elements and TOC in core VR-1A with defined zones. Gray-shaded backgrounds show climatic events during the late Glacial and Holocene periods. Temperatures are from the Greenland ice core (GISP-2, [65]) and sea surface temperature from the Adriatic Sea (SSR April-May, [64]). Estimated sea level (esl) curve is projected from [31].

 doi:10.20944/preprints202408.2193.v1

4.1.3. . Early to Middle Holocene (11.7-4.4 cal kyr BP; Zones 5 and 6)

The early Holocene (11.7 cal kyr BP, 3.00 m) up to 10.0 cal kyr BP (2.50 m) is marked by the increase in siliciclastic input, which is the highest in the middle Holocene between 10.0 and 4.4 cal kyr BP (2.50-1.25 m). High organic carbon content (~4%) appears in the period 10.7-10.0 cal kyr BP (2.70-2.50 m), with a higher C/N ratio, indicating a significant contribution of terrigenous organic matter to the lake. TOC values from 10.0 to 8.0 cal kyr BP are a bit higher (~2.4%) compared to the period 8.0-4.4 cal kyr BP where it has a value of 1.4%), but both are dominated by algal organic matter (C/N values 7-9). The timing of the increased precipitation coincides with the formation of organic-rich layers of sapropel (S1a, S1b) deposited in the eastern and central Mediterranean [62,64,73,74].

The sea level at ~10 kyr BP (~40 m lower than today), could have affected the rise of lake level in Lake Vrana. During this time the sea surrounded the Island of Cres (Figure 14C). The seawater flooded nearby Lošinj Channel through sill at 10.5 cal kyr BP [16].

The highest magnetic susceptibility and siliciclastic elements between 8.0 cal kyr BP and 4.9 cal kyr BP (1.90-1.34 m), indicate erosion of the siliciclastic material from the catchment and terrigenous supply of mainly siliciclastic elements, with less dolomite entering the lake (Mg/Ca indicates that Mg derives from clay minerals). In the Adriatic basin, the periods at 7.7 kyr BP and between 7.5-7 kyr BP are defined as the maximum of the summer precipitation and increased sediment input into the Adriatic Sea occurred [75]. Increased precipitation is thought to be linked to increased rainfall over the Mediterranean region [76,77]. The enhanced regional rainfall is detected between 8.9 and 7.3 kyr BP, with the peak between 7.9 and 7.4 kyr BP, in central Italy (Corchia cave [78]). Freshwater discharge is recorded in Lake Veliko jezero on the Island of Mljet, where the wet climate phase coincides with the occurrence of Mg-calcite in the lake and its predominance over aragonite from 7.6 to 7 kyr BP [21,23]. Here, the wet, pluvial phase extends to a longer period, induced by the geomorphological characteristics of the steep slopes on the eastern and western lake shores, while on the southern shore with a gentler relief alluvial fan is formed, which is intersected by the temporary incisions and stream/river beds, that can bring a significant amount of material into the lake. The material deposited in the lake from the beginning of the Holocene shows a similar clay mineral assemblage to the base of the core (chlorite, hydroxy-interlayered vermiculite, illite, and kaolinite), although they differ significantly in dolomite content. These clay minerals were present in Holocene sediments, which have lower amounts of dolomite. However, dolomite is the only carbonate mineral present in these sediments.

This interval was also documented in [7], with quartz and clay minerals present, and the absence of calcite. They assumed that this is the result of calcite dissolution, possibly by CO_2-enriched cold waters [7]. Indeed, the solubility of calcite increases with decreasing water temperature [6], and decreasing pH as the result of the decomposition of organic matter which also leads to the formation of CO_2, and calcite dissolution [5].This means that the endogenic calcite, formed in the photosynthetic zone of hardwater lakes due to the CO_2 consumption of algae or macrophytes, doesn't necessarily reach the lake bottom in the deeper lake. Calcite comes in contact with cold water due to the thermocline formation. Possibly, this was the period when thermal stratification during summer months was established in the lake. During this period, increased precipitation provided freshwater discharge and promoted strong stratification of the water column, recorded in the central Mediterranean [71].

According to [7], during this interval (1.8-1.2 m; mid-Holocene) Lake Vrana may have reached its present depth. Based on the sediment core CS-9 record, the carbonate sedimentation in the lake environment is determined from 3.3 cal kyr BP. As the core is located at the edge of the lake, at 13 m a.s.l., it is proposed that the present lake level was not established before 3.3 cal kyr BP (1.4 m core depth). Based on the record from the sediment core CS-5, located at 15 m a.s.al., carbonate sedimentation did not occur, which means that the lake level was never higher than 15 m a.s.l.

4.1.4. . Late Holocene (4.4 cal kyr BP to Present; Zones 7 to 10)

Late Holocene sediments are divided into four distinct periods of deposition: 4.4-1.6 cal kyr BP, 1.6-0.4 cal kyr BP, 0.4-0.1 cal kyr BP and the last 100 years.

 doi:10.20944/preprints202408.2193.v1

The beginning of the late Holocene (4.4-1.6 cal kyr BP, 1.25-0.70 m) is marked by the presence of highly organic sediments, which are characterized by the increased TOC content (3.4-8.2%), similar to the values of late Glacial to Holocene transition sediments. The siliciclastic material is still significant, although with a decreasing trend. In the opposite, Ca and TIC values are increasing, especially in the upper part of the zone. The C/N ratio is relatively constant throughout the zone, with values of ~8, which is slightly lower than the older organic sediments (>10). This fact highlights the difference in the origin of organic carbon during different paleoenvironmental phases. In this period, C/N ratios are typically lower than 10 and indicate a greater contribution of lake phytoplankton [79] and higher lake productivity. The endogenic calcite precipitated in this highly productive lake, with intensive photosynthesis and increasing pH. The calcite was probably partially dissolved at the beginning of the zone, due to the high TOC and organic matter content. It is dissolved when settling to the hypolimnion or the lake bottom since the pH is always lower due to the decomposition of organic matter. Another possibility for calcite dissolving is due to the change in thermocline depth, which shallowing is shown to be the main reason for organic carbon preservation in Lake Veliko jezero during a cold and dry climate that promoted anoxic conditions [23].

Increased carbonate, i.e. endogenic calcite sedimentation is evident in the period between 1.6-0.4 cal kyr BP (0.70-0.20 m). Siliciclastic material and TOC contents are lower than in the previous zone (1.2-2.1%). Mg comes mainly from calcite (low Mg/Al ratio). This marks typical carbonate sedimentation in karstic lakes, with endogenic calcite precipitation as the result of calcite supersaturation, and formation of deeper water lake conditions.

In the last 400 years (0.20-0.04 m), there has been a shift to the deposition of siliciclastic material, caused by input and erosion from the catchment. This event could be attributed to the Little Ice Age (LIA) period, with enhanced precipitation and sediment discharge from the catchment. This more humid phase is evidenced in Lake Veliko Blato [12], Lake Butrint [80] and Lake Dojran [81,82], in the central Mediterranean. The TOC values are higher (4-5%), and the C/N ratio indicates aquatic organic matter, as a result of lake productivity. There are evident two peaks of Pb (normalized to Al in Figure 14), first at 1.6 cal kyr BP, and second peak appears at 400 cal kyr BP. Both could be correlated to the previously higher Pb record in Lake Vrana sediments [29], derived from anthropogenic sources, during Roman and modern periods, respectively. This period is correlated to increased allochthonous influx from human catchment disturbances [7]. Pb has been identified in sediments as an atmospheric pollutant [83,84].

The last 100 years (0.04-0 m) have been marked by decreasing input of siliciclastic material and higher Ca content. The re-establishment of dominant calcite precipitation indicates stable lake levels. Since most of the soil cover was transported into the lake during LIA and the soil erosion was exhausted by the year 1771, as the area around the lake was described by the Italian traveler Fortis as a “stone desert” [85]. The vegetation in the catchment has been recovering over the past 50 years because of the water protection measures enforced for the protection of the lake as a source of potable water for the islands of Cres and Lošinj.

4.2. Deciphering Sediment Source for Lake Vrana Sediments

Sediment cores from the alluvial fan in the southern part of the lake shore have been collected to possibly identify sediment source material. The comparison of lake sediments from core VR-1A, deposited in different time intervals, to sediments from cores CS-5 and CS-9, as well as profile CS-P, yielded that dolomite content plays a significant role. This is shown in the Mg to Ca concentrations scatterplots (Figure 15A), where the highest Mg and resulting dolomite content in the core VR-1A are evident in the oldest Late Pleistocene sediments (>40 kyrs BP) from core VR-1A and are similar to sediments from CS-P, with significant dolomite content. The sediments from 16.4-14.4 cal kyr BP that contain a significant amount of dolomite and Mg, are located towards dolomite group of sediments, and are similar only to the sediments deposited between 13.3-12.7 cal kyr BP. In this line, the youngest sediments (3.3-0 cal kyr BP) from core CS-9 appear, as well as the youngest sediments from CS-5, with high dolomite content and no calcite present.

 doi:10.20944/preprints202408.2193.v1

Using the Na to Al concentrations scatterplot of analyzed samples (Figure 15B), eroded sediments from CS-9 in the period 7.5-7.3 cal kyr BP and partially 7.3-3.3 cal kyr BP overlap with the eroded sediments from core CS-5 in the period 8.2-7.0 cal kyr BP (blue circle). Sediments from CS-5 deposited in the period 7.0-2.4 cal kyr BP show similar composition to VR-1A sediments deposited between 11.7-10.0 cal kyr BP and 10.0-4.4 cal kyr BP (red circle). Increased Na concentrations of sediments from VR-1A deposited in the period 14.4-13.3 cal kyr BP, which could originate from basaltic rocks from the Velebit Mt. [72], are located in line towards the blue circle. These sediments showed a more clayey composition, which supports the hypothesis of wind-blown material.

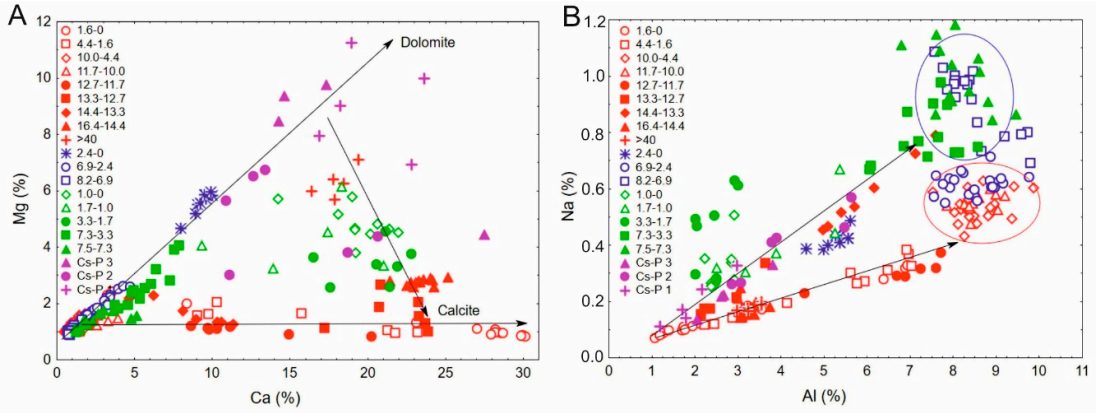

Figure 15. Scatterplots of the Mg to Ca (left) and Na to Al (right) ratios in the sediment cores (VR-1A red color, CS-5 blue color, CS-9 green color) and profile CS-P (purple color).

Clay minerals in Lake Vrana sediments from the VR-1A core are detrital and reveal the two different compositions (Figure 16). The clay mineral assemblage of the oldest Late Pleistocene and Holocene sediments from core VR-1A (chlorite, hydroxy-interlayered vermiculite, illite and kaolinite) is recorded in Holocene sediments in cores CS-5 and CS-9 from alluvial fan on the southern shores of the lake. This corresponds to the composition of terra rossa/red soils in the catchment (Valun sample, without dolomite). Hydroxy inter-stratified minerals (HIM) are common mixed layer minerals in soils [86], and are considered transition minerals during the alteration of chlorite to smectite [87], and they form through the polymerization of Al-hydroxides in the interlayer, which frequently encounters in moderately acidic soils [86]. The transformation of clay minerals in acidic soils is related to the transition of chlorite and illite into swelling clay minerals, vermiculite and smectite, which often contain hydroxy interlayers and are often called „soil vermiculite“ [86,88]. Terra rossa is a red soil-sediment overlying carbonate rocks, widespread in the Croatian karst, and is considered as a polygenetic paleosol [89,90]. The clay mineral assemblage of Istrian terra rossa kaolinite and illite dominate, with the presence of chlorite and vermiculite [89], while in red paleosols smectite also appears [91]. In comparison, Pleistocene loess from NW Istria, contains additionally, low-charge-vermiculite or high-charge smectite and mixed-layer clay minerals (other than illitic material) [89].

The source of clays (smectite, chlorite, illite, and kaolinite) in Lake Vrana sediments deposited during the transition from the late Glacial to Holocene period (16.6-11.7 cal kyr BP) corresponds to the composition of the loess-like material in profile CS-P, which contains swelling clay minerals (smectite and illite-smectite), in addition to chlorite and kaolinite. Loess and loess-like deposits are locally present in the surrounding area (islands Krk, Lošinj, Unije), the most significant is a 90-m-thick loess-paleosol sequence on the Island of Susak, in the vicinity of the Island of Cres, dated to MIS 3 [92], which showed the presence of smectite and illite-smectite mixed-layer mineral, especially in the youngest loess material dated to 16.1 ka [92,93]. In general, late Glacial loess contains smectite, which is not present in polygenetic soil [93], which supports the source of loess-like material for sediments from CS-P profile and late Glacial Lake Vrana sediments (16.4.-11.7 cal kyr BP).

 doi:10.20944/preprints202408.2193.v1

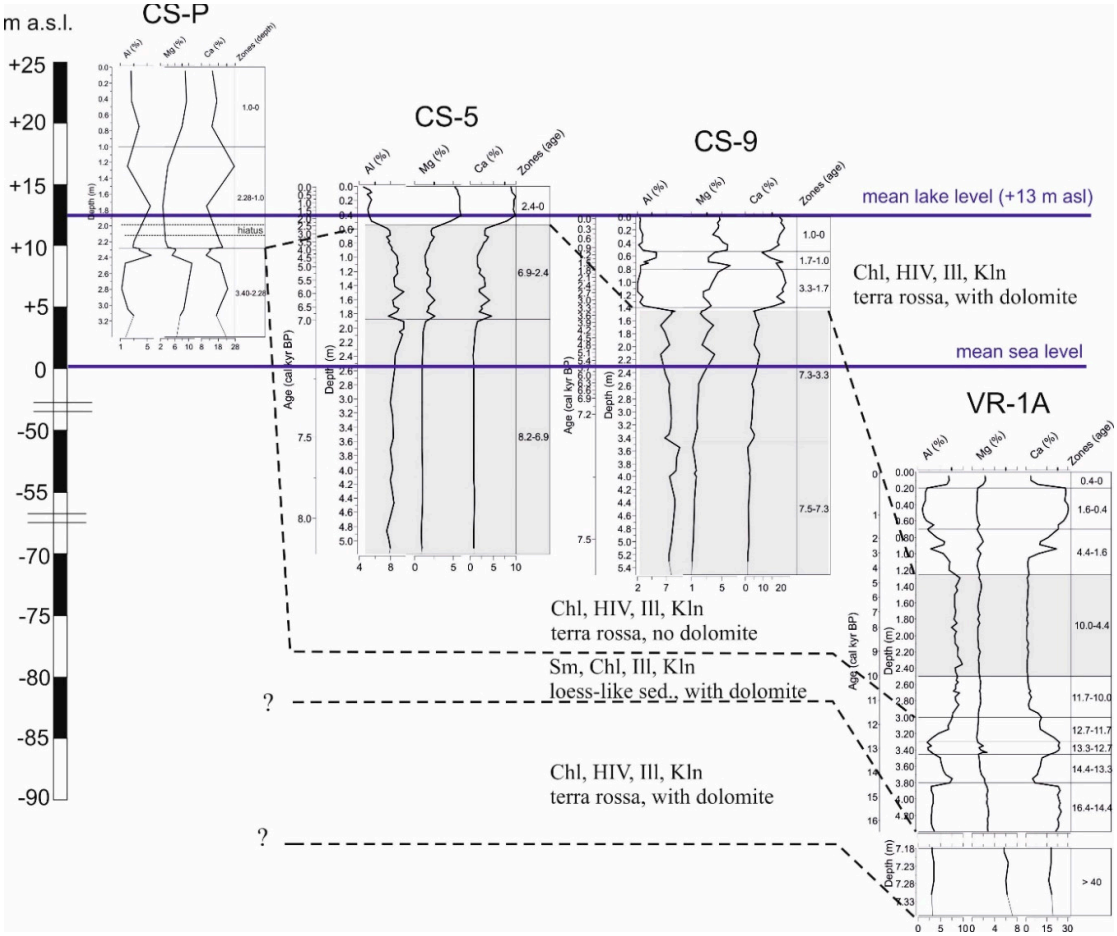

Figure 16. The main geochemical elements (Al, Mg, and Ca) with clay mineralogical composition in sediments from CS-P, CS-5, CS-9, and VR-1A and marked possible source material based on clay mineral assemblages. Note that the core depths are not on the same scale as the altitude on the left side.

Therefore, the clay minerals in Lake Vrana indicate the origin of the material and the sediment source available at different periods. They are related to sediment erosion and the delivery of detrital siliciclastic material, which was subjected to pedogenesis. Kaolinite is in all samples present as both well-crystallized (ordered, which forms intercalation compound with DMSO), and poorly-crystallized clay minerals phase (disordered, which doesn't form the intercalation compound with DMSO). The latter is present as the dominant mineral phase in the clay fraction of Istrian terra rossa [89] and is considered pedogenic kaolinite.

5. Conclusions

The paleolimnological research of Lake Vrana on the island of Cres is based on sediment core VR-1A (7.4 m) from the central part of the lake, which contains more than 25 m of lake sediments, and two sediment cores and profiles from the alluvial fan in the southern part of the lake shore. This lake is the deepest freshwater lake in Croatia (avg. 54-55 m; 41-42 m b.s.l.) with a relatively small surface area of 5.75 km^2, a mean lake level of 13.1 m a.b.l. It is an oligotrophic closed lake without permanent surface inflow or outflow. Its location in the center of the island of Cres, close to the sea in the karstic region of the eastern Adriatic coast, is assumed to be affected by seawater. In contrast, the lake has been used for public water supply for more than half of the century, owing to the excellent quality of freshwater. Even with high abstraction rates during intensive pumping, the lake water was not affected by seawater; therefore, this connection was excluded. The extreme use of lake

 doi:10.20944/preprints202408.2193.v1

water impacted the lake level and caused it to drop to its lowest point at 9.11 m b.s.l. in 1990. Since then, the lake level has been regulated, monitored, and maintained at 11-12 m a.s.l. [35].

The recovered sediment core VR-1A, with a total length of 7.4 m, contains continuously deposited lake sediments, without evidence of a terrestrial environment that would imply the development of a karst polje phase. The oldest sediments in Lake Vrana (7.4-4.4 m) are proposed to be older than 40 kyrs and could be deposited during the MIS 3 period, as evidenced by similar seismic reflectors in Lošinj Channel lake phase (Lošinj paleolake MIS 3: 46.5-44.7 cal kyr BP) [16].

Sediments deposited from the period between 16.4 and 14.4 cal kyr BP (4.4-3.8 m) are characterized by a higher amount of calcite, dolomite is also present in significant amount, while in clay minerals fraction smectite appears, which is present in loess-like material in the catchment, alongside illite and kaolinite. Siliciclastic material is increasing in the lake sediments between 14.4 and 11.7 cal kyr BP (3.8-3.0 m), with high sand and TOC content. The apparent "interruption" interval between 13.3-12.7. cal kyr BP (3.45-3.3 m), evident in bright, carbonate sediments with low TOC values, could be interpreted as turbiditic sediments derived from lake-littoral to the relatively shallow lake. The sediments from the lower section of this unit, contain a high content of Na compared to the upper section and indicate different source material. The entire late Glacial to Holocene transition period is marked by enhanced erosion caused by the humid period and higher precipitation. However, low lake levels prevailed due to the general low sea level and the water loss through the karst and groundwater. The beginning of the Holocene (3.0 m) is characterized by the deposition of siliciclastic material (high values of Al and other detrital elements, quartz and feldspars recorded in sediments), which is continued into the middle Holocene, until 4.4 cal kyr BP (1.25 m). Enhanced input and erosion of siliciclastic material is the highest in the period between 8.0 cal kyr BP and 4.9 cal kyr BP, indicating higher precipitation marked as pluvial period. Late Holocene is marked by sediments that underwent changes between calcite-rich (i.e. deeper stable lake) and siliciclastic-dominated (i.e. high-inflow lake) conditions. Higher TOC content, decreasing trend in siliciclastic material content and increasing trend in Ca and TIC contents from 4.4 to 1.6 cal kyr BP mark the high productivity lake. Dominant calcite sedimentation indicates the development of the deeper lake from 1.6 to 0.04 cal kyr BP. In the last 400 years, it is evident that increased erosion and sediment run-off in the basin, manifest in higher siliciclastic material, which could be attributed to LIA. The re-establishment of calcite sedimentation is observed in the last 100 years.

The clay mineral assemblage in the Holocene sediments (chlorite, hydroxy interlayered vermiculite, illite and kaolinite) is similar to the Late Pleistocene sediments from the base of the core, and could reflect the same sediment source of terra rossa soils present in the catchment, while late Glacial sediments (16.4-11.7 cal kyr BP) show similar clay mineral assemblage to loess-like sediments (smectite, illite-smectite) from the catchment.

This study gave a chronological framework of the lake sediments in Lake Vrana, covering the Holocene sediments in 3-m-thick succession and 4-m-thick lake sediments that correspond to the Late Pleistocene period, in more than 25 m of the sediment infill, which evidence lake sedimentation for at least 40 kyrs BP in Lake Vrana karstic cyptodepression.

Supplementary Materials: The following supporting information can be downloaded at the website of this paper posted on Preprints.org, Supplementary file S1: Geochemical analysis from all analyzed sediment cores (VR-1A, CS-5, CS-9, CS-P, VJ-8 and VJ-10).

Author Contributions: Conceptualization, N.I. and S.Mi.; resources, S. Mi. and S.Me.; writing—original draft preparation, N.I. and S.Me.; writing—review and editing, S.Mi., O.H., D.B.; methodology, S.Mi., N.I., M.Š.M.; funding acquisition, S.Mi. and S.Me. All authors have read and agreed to the published version of the manuscript.

Funding: This research was funded by the Ministry of Science and Education of the Republic of Croatia (project number 181-1953068-0363), by the EU project from SEE Cooperation Program (project CC-WaterS), and by the Croatian Waters (Hrvatske vode) contract number 974/2006.

Data Availability Statement: The data presented in this study are available on request from the corresponding author.

Acknowledgments: This work was funded by the project "Holocene sediments as archives of environmental change in the Adriatic catchments", funded by the Ministry of Science and Education of the Republic of Croatia and EU-funded project (SEE Cooperation Program) "Climate change and impact on water supply (CC-WaterS)". We are grateful to Croatian Waters (Hrvatske vode), for continuing to support scientific research of Lake Vrana on the Island of Cres. We are greatly thankful to colleagues who assisted during fieldwork campaign with platform, Hana Fajković, Filip Presečki and Domagoj Živković, as well as with drilling on the shore of the lake and core sub-sampling, Erli Kovačević Galović and Željko Dedić. We thank to Helena Ćućuzović for grain size analysis and Tamara Marković for chemical analysis of lake water.

Conflicts of Interest: The authors declare no conflicts of interest.

References

1. Roberts, N.; Jones, M. D.; Benkaddour, A.; Eastwood, W. J.; Filippi, M. L.; Frogley, M. R.; Lamb, H. F.; Leng, M. J.; Reed, J. M.; Stein, M.; Stevens, L.; Valero-Garcés, B.; Zanchetta, G. Stable Isotope Records of Late Quaternary Climate and Hydrology from Mediterranean Lakes: The ISOMED Synthesis. Quat. Sci. Rev. 2008, 27 (25–26), 2426–2441. https://doi.org/10.1016/j.quascirev.2008.09.005.
2. Kuhta, M.; Brkić, Ž. Seasonal Temperature Variations of Lake Vrana on the Island of Cres and Possible Influence of Global Climate Changes. J. Earth Sci. Eng. 2013, 4, 225–237.
3. Brkić, Ž. Increasing water temperature of the largest freshwater lake on the Mediterranean islands as an indicator of global warming. e19248 Heliyon 2023, 9 (8). https://doi.org/10.1016/j.heliyon.2023.e19248
4. Hrnjica, B.; Bonacci, O. Lake Level Prediction using Feed Forward and Recurrent Neural Networks. Water Resour. Manage. 2019, 33, 2471-2484. https://doi.org/10.1007/s11269-019-02255-2.
5. Last, W. M.; Smol, J. P. An Introduction to Physical and Geochemical Methods Used in Paleolimnology. In Tracking Environmental Change Using Lake Sediments; Last, W. M., Smol, J. P., Eds.; Kluwer Academic Publishers: Dordrecht, 2001; pp 1–5. https://doi.org/10.1007/0-306-47670-3_1.
6. Håkanson, L.; Jansson, M. Principles of lake sedimentology, The Blackburn Press, USA, 2002.
7. Schmidt, R.; Müller, J.; Drescher-Schneider, R.; Krisai, R.; Szeroczyńska, K.; Barić, A. Changes in Lake Level and Trophy at Lake Vrana, a Large Karstic Lake on the Island of Cres (Croatia), with Respect to Palaeoclimate and Anthropogenic Impacts during the Last Approx. 16,000 Years. J. Limnol. 2000, 59 (2), 113. https://doi.org/10.4081/jlimnol.2000.113.
8. Bakrač, K.; Ilijanić, N.; Miko, S.; Hasan, O. Evidence of Sapropel S1 Formation from Holocene Lacustrine Sequences in Lake Vrana in Dalmatia (Croatia). Quat. Int. 2018, 494, 5–18. https://doi.org/10.1016/j.quaint.2018.06.010.
9. Caput Mihalić, K.; Galović, I.; Ilijanić, N.; Hasan, O.; Ledinski, M.; Miko, S.; Mesić, S. Evidence of lake-level fluctuations during the late Holocene based on diatoms from Lake Vransko, Cres Island (north-central Mediterranean). Quat. Int. 2024. https://doi.org/10.1016/j.quaint.2024.06.004 (in press).
10. Galović, I.; Caput Mihalić, K.; Ilijanić, N.; Miko, S.; Hasan, O. Diatom Responses to Holocene Environmental Changes in a Karstic Lake Vrana in Dalmatia (Croatia). Quaternary International. 2018, 67–179. https://doi.org/10.1016/j.quaint.2017.09.010.
11. Hajek-Tadesse, V.; Ilijanić, N.; Miko, S.; Hasan, O. Holocene Ostracoda (Crustacea) from the Shallow Lake Vrana (Dalmatia, Croatia) and Their Paleoenvironmental Significance. Quat. Int. 2018, 494, 80–91. https://doi.org/10.1016/j.quaint.2018.01.007
12. Ilijanić, N.; Miko, S.; Ivkić Filipović, I.: Hasan, O., Šparica Miko, M.; Petrinec, B., Terzić, J.; Marković, T. A Holocene Sedimentary Record and the Impact of Sea-Level rise in the Karst Lake Velo Blato and the Wetlands on Pag Island (Croatia). Water. 2022, 14, 342. https://doi.org/10.3390/w14030342.
13. Balbo, A.L.; Andrič, M.; Rubinić, J., Moscariello, A., Miracle, P.T. Palaeoenvironmental and archaeological implications of a sediment core from Polje Čepić, Istria, Croatia. Geol. Croat. 2006. 59/2, 109–124. https://doi.org/10.4154/GC.2006.08
14. Ilijanić, N.; Miko, S.; Hasan, O.; Bakrač, K. Holocene Environmental Record from Lake Sediments in the Bokanjačko Blato Karst Polje (Dalmatia, Croatia). Quat. Int. 2018, 494, 66–79. https://doi.org/10.1016/j.quaint.2018.01.037.
15. Schmidt, R.; Pugliese, N.; Müller, J.; Szeroczyriska, K.; Bogner, D.; Melis, R.; Kamenik, C.; Bari, A.; Danielopol, D.L. Palaeoclimate, vegetation and coastal lake development, from the Pleniglacial until early Holocene, in the northern Adriatic Valun bay (Isle of Cres, Croatia). J. Quat. Sci. 2001, 14, 61–78.

16. Brunović, D.; Miko, S.; Hasan, O.; Papatheodorou, G.; Ilijanić, N.; Miserocchi, S.; Correggiari, A.; Geraga, M. Late Pleistocene and Holocene Paleoenvironmental Reconstruction of a Drowned Karst Isolation Basin (Lošinj Channel, NE Adriatic Sea). Palaeogeogr. Palaeoclimatol. Palaeoecol. 2020, 544. https://doi.org/10.1016/j.palaeo.2020.109587
17. Brunović, D.; Hasan, O.; Miko, S.; Georgiou, N., Geraga, M., Christodoulou, D.; Dimas, X.; Ilijanić, N.; Papatheodorou, G. High-resolution seismic record of the Quaternary palaeoenvironments along a Dalmatian-type coast (Lošinj Channel, Adriatic Sea). Mar. Geol. 2024, 474, 107325. https://doi.org/10.1016/j.margeo.2024.107325.
18. Šolaja, D.; Miko, S.; Brunović, D.; Ilijanić, N.; Hasan, O.; Papatheodorou, G.; Geraga, M.; Durn, T.; Christodoulou, D.; Razum, I.; Late Quaternary Evolution of a Submerged Karst Basin Influenced by active Tectonics (Koločep Bay, Croatia). J. Mar. Sci. Eng. 2022, 10, 881. https://doi.org/10.3390/jmse10070881.
19. Jahns, S.; Bogaard, C. New palynological and tephrostratigraphical investigations of two salt lagoons on the island of Mljet, south Dalmatia, Croatia. Veg. Hist. Archaeobotany 1998, 7 (4), 219–234. https://doi.org/10.1007/BF01146195.
20. Wunsam, S.; Schmidt, R.; Müller, J. Holocene Lake Development of Two Dalmatian Lagoons (Malo and Veliko Jezero, Isle of Mljet) in Respect to Changes in Adriatic Sea Level and Climate. Palaeogeogr. Palaeoclimatol. Palaeoecol. 1999, 146 (1–4), 251–281. https://doi.org/10.1016/S0031-0182(98)00147-3
21. Razum, I.; Miko, S.; Ilijanić, N.; Hasan, O.; Šparica Miko, M.; Brunović, D.; Pawlowsky-Glahn, V. A Compositional Approach to the Reconstruction of Geochemical Processes Involved in the Evolution of Holocene Marine Flooded Coastal Karst Basins (Mljet Island, Croatia). Appl. Geochemistry 2020, 116, 104574. https://doi.org/10.1016/j.apgeochem.2020.104574.
22. Razum, I.; Miko, S.; Ilijanić, N.; Petrelli, M.; Röhl, U.; Hasan, O.; Giaccio, B. Holocene Tephra Record of Lake Veliko Jezero, Croatia: Implications for the Central Mediterranean Tephrostratigraphy and Sea Level Rise. Boreas 2020, 49 (3), 653–673. https://doi.org/10.1111/bor.12446.
23. Razum, I.; Bajo, P.; Brunović, D.; Ilijanić, N.; Hasan, O.; Röhl, U.; Miko, M. Š.; Miko, S. Past Climate Variations Recorded in Needle-like Aragonites Correlate with Organic Carbon Burial Efficiency as Revealed by Lake Sediments in Croatia. Sci. Rep. 2021, 11 (1), 7568. https://doi.org/10.1038/s41598-021-87166-2.
24. Hasan, O.; Miko, S.; Brunović, D.; Papatheodorou, G.; Christodolou, D.; Ilijanić, N.; Geraga, M. Geomorphology of Canyon Outlets in Zrmanja River Estuary and Its Effect on the Holocene Flooding of Semi-Enclosed Basins (the Novigrad and Karin Seas, Eastern Adriatic). Water 2020, 12 (10), 2807. https://doi.org/10.3390/w12102807.
25. Hasan, O.; Smrkulj, N.; Miko, S.; Brunović, D.; Ilijanić, N.; Šparica Miko, M. Integrated Reconstruction of late Quaternary Geomorphology and Sediment Dynamics of Prokljan Lake and Krka River Estuary, Croatia. Remote Sens. 2023, 15, 2588. https://doi.org/10.3390/rs15102588.
26. Smrkulj, N.; Hasan, O.; Brunović, D., Miko, S.; Ilijanić, N. Holocene palaeoenvironmental development of Prokljan Lake (Krka River, Croatia): Evolution from a calcareous tufa barrier system to a karst estuary. Mar. Geol. 2024, 476, 107370. https://doi.org/10.1016/j.margeo.2024.107370
27. Ford, D.; Williams, P. Karst Hydrogeology and Geomorphology; John Wiley & Sons Ltd.: Chichester, UK, 2007.
28. Miko, S., Mesić, S., Prohić, E. i Peh, Z. Trace element distribution in surface sediments of Lake Vrana and topsoil of Cres island, Croatia. Natura Croatica. 2003, 12/2, 93–111. https://hrcak.srce.hr/11458
29. Miko, S., Mesić, S., Šparica Miko, M., Hasan, O. A record of anthropogenic Pb deposition in a Mediterranean karst catchment (Lake Vrana, Cres Island, Croatia). Mineralogical Magazine. 2008, 72/1, 455–460. doi:10.1180/minmag.2008.072.1.455
30. Waelbroeck, C.; Labeyrie, L.; Michel, E.; Duplessy, J.C.; McManus, J.F.; Lambeck, K.; Balbon, E.; Labracherie, M. Sea-level and deep water temperature changes derived from benthic foraminifera isotopic records. Quat. Sci. Rev. 2002, 21, 295–305. https://doi.org/10.1016/S0277-3791(01)00101-9.
31. Lambeck, K.; Rouby, H.; Purcell, A.; Sun, Y.; Sambridge, M. Sea Level and Global Ice Volumes from the Last Glacial Maximum to the Holocene. Proc. Natl. Acad. Sci. 2014, 111 (43), 15296–15303. https://doi.org/10.1073/pnas.1411762111.
32. Benjamin, J.; Rovere, A.; Fontana, A.; Furlani, S.; Vacchi, M.; Inglis, R. H.; Galili, E.; Antonioli, F.; Sivan, D.; Miko, S.; Mourtzas, N.; Felja, I.; Meredith-Williams, M.; Goodman-Tchernov, B.; Kolaiti, E.; Anzidei, M.; Gehrels, R. Late Quaternary Sea-Level Changes and Early Human Societies in the Central and Eastern

 doi:10.20944/preprints202408.2193.v1

Mediterranean Basin: An Interdisciplinary Review. Quat. Int. 2017, 449, 29–57. https://doi.org/10.1016/J.QUAINT.2017.06.025.

33. Pikelj, K.; Juračić, M. Eastern Adriatic Coast (EAC): Geomorphology and Coastal Vulnerability of a Karstic Coast. J. Coast. Res. 2013, 289, 944–957. https://doi.org/10.2112/JCOASTRES-D-12-00136.1.
34. Leder, T.D.; Ujević, T.; Čala, M. Coastline Lenghts and Areas of Islands in the Croatian Part of the Adriatic Sea Determined from the Topographic Maps at the Scale of 1:25,000. Geoadria 2017, 9, 5–32.
35. Brkić, Ž.; Kuhta, M. Lake level evolution of the largest freshwater lake on the Mediterranean islands through drought analysis and machine learning. Sustainability. 2022, 14, 10447. https://doi.org/10.3390/su141610447
36. Fuček, L.; Matičec, D.; Vlahović, I.; Oštrić, N.; Prtoljan, B.; Korbar, T.; Husinec, A.; Palenik, D. Basic Geological Map of the Republic of Croatia Scale 1:50.000 - Sheet Cres 4. Croatian Geological Survey, Zagreb. 2014.
37. Korbar, T. Orogenic evolution of the External Dinarides in the NE Adriatic region: a model constrained by tectonostratigraphy of Upper Cretaceous to Palaeogene carbonates. Earth-Sci. Rev. 2009, 96 (4), 296–312. https://doi.org/10.1016/j.earscirev.2009.07.004
38. Vlahović, I.; Tišljar, J.; Velić, I.; Matičec, D. Evolution of the Adriatic Carbonate Platform: Palaeogeography, Main Events and Depositional Dynamics. Palaeogeogr. Palaeoclimatol. Palaeoecol. 2005, 220, 333–360.
39. Bonacci, O. The Vrana Lake Hidrology (Island of Cres-Croatia), Journal of the American Water Resources Association. 1993. 29/3, 407–417.
40. Hertelendi E, Svingor E, Futo I, Szanto Zs.; Rank D. Isotope Investigation of Lake Vrana and Springs in the Kvarner Area. Rapid Communication in Mass Spectrometry 1997, 11, 651-5.
41. Brkić, Ž.; Larva, O. Impact of climate change on the Vrana Lake surface water temperature in Croatia using support vector regression. Journal of Hydrology: Regional Studies. 2024, 54, 101858. https://doi.org/10.1016/j.ejrh.2024.101858.
42. Ožanić, N. Hydrological Functioning Model of the Vrana Lake on the Cres Island. Ph.D. Thesis, University of Split, Split, Croatia, 1996. [In Croatian].
43. Koeck, R. CC-WaterS Monograph. Climate Change and Impact on Water Supply, Vienna. 2012.
44. Gligora Udovič, M.; Žutinić. P.; Kralj Borojević, K.; Plenković-Moraj, A. Co-occurrence of functional groups in phytoplankton assemblages dominated by diatoms, chrysophytes and dinoflagellates. Fundamental and Applied Limnology. 2015, 187, 101–111. 10.1127/fal/2015/0759
45. Gligora Udovič, M.; Cvetkoska, A.; Žutinić. P.; Bosak, S.; Stanković, I.; Špoljarić, I.; Mršić, G.; Kralj Borojević, K.; Čukurin, A.; Plenković-Moraj, A. Defining centric diatoms of most relevant phytoplankton functional groups in deep karst lakes. Hydrobiologia. 2017. 78: 169–191. https://doi.org/10.1007/s10750-016-2996-z
46. Golubić, S. Prethodna istraživanja vegetacije jezera Vrana na otoku Cresu. Ljetopis JAZU, 1961. Book 65, Zagreb, 295-297.
47. Alegro, A.; Stanković, I.; Šegota, V.; Van de Weyer; Blaženčić, J. Macrophytic vegetation in the oligotrophic Mediterranean Lake Vrana (Island of Cres, Northern Adriatic) – New insight after 50 years. Botanica Serbica. 2016. 40 (2), 137144.
48. Blott, S. J.; Pye, K. GRADISTAT. A Grain Size Distribution and Statistics Package for the Analysis of Unconsolidated Sediments. Earth Surf. Process. Landforms 2001, 26 (11), 1237–1248. https://doi.org/10.1002/esp.261
49. Juggins, S. C2 data analysis, version 1.7.4., software for ecological and palaeooecological dana analysis and visualisation, Newcastle University, Newcastle upon Tyne, UK. 2011.
50. Brindley, G.W.; Brown, G. Crystal structures of clay minerals and their X-ray identification. Mineralogical Society, London, 1980.
51. Moore, D. M.; Reynolds, R. C. X-Ray Diffraction and the Identification and Analysis of Clay Minerals, second.; Oxford University Press: Oxford, 1997.
52. Döbelin, N. Profex, version 3.0.0. RMS Foundation, Bettlach, Switzerland. 2013.
53. Van der Weijden, C.H. Pitfalls of normalization of marine geochemical data using a common divisor. Mar. Geol. 2002, 184/3-4, 167–187. https://doi.org/10.1016/S0025-3227(01)00297-3
54. StatSoft, Inc. (2006). STATISTICA (Data Analysis Software System), Version 7.1. www. 739 statsoft.com2006.

 doi:10.20944/preprints202408.2193.v1

55. Reimer, P., Austin, W., Bard, E., Bayliss, A., Blackwell, P., Bronk Ramsey, C., Butzin, M., Cheng, H., Edwards, R., Friedrich, M., Grootes, P., Guilderson, T., Hajdas, I., Heaton, T., Hogg, A., Hughen, K., Kromer, B., Manning, S., Muscheler, R., Palmer, J., Pearson, C., van der Plicht, J., Reimer, R., Richards, D., Scott, E., Southon, J., Turney, C., Wacker, L., Adolphi, F., Büntgen, U., Capano, M., Fahrni, S., Fogtmann-Schulz, A., Friedrich, R., Köhler, P., Kudsk, S., Miyake, F., Olsen, J., Reinig, F., Sakamoto, M., Sookdeo, A., & Talamo, S. The IntCal20 Northern Hemisphere radiocarbon age calibration curve (0–55 cal kBP). Radiocarbon. 2020, 62.
56. Blaauw, M. Methods and code for 'classical' age-modelling of radiocarbon sequences. Quaternary Geochronology. 2010, 5, 512–518.
57. Balsam W.L.; Deaton, B.C.; Damuth, J.E. Evaluating optical lightness as a proxy for carbonate content in marine sediment cores, Marine Geology. 1999, 161, 141-153.
58. Maher, B.A.; Thompson, R. Quaternary Climates, Environments and Magetism. Cambridge University Press, 1999..
59. Antonioli, F.; Ferranti, L.; Fontana, A.; Amorosi, A.; Bondesan, A.; Braitenberg, C.; Dutton, A.; Fontolan, G.; Furlani, S.; Lambeck, K.; Mastronuzzi, G.; Monaco, C.; Spada, G.; Stocchi, P. Holocene relative sea-level changes and vertical movements along the Italian and Istrian coastlines. Quat. Int. 2009. 206, 102–133. https://doi.org/10.1016/j.quaint.2008.11.008.
60. Maselli, V.; Hutton, E.W.; Kettner, A.J.; Syvitski, J.P.M.; Trincardi, F. Highfrequency Sea level and sediment supply fluctuations during termination I: an integrated sequence-stratigraphy and modeling approach from the Adriatic Sea (Central Mediterranean). Mar. Geol. 2011. 287, 54–70. https://doi.org/10.1016/j.margeo.2011.06.012.
61. Maselli, V.; Trincardi, F. Large-scale single incised valley from a small catchment basin on the western Adriatic margin (Central Mediterranean Sea). Glob. Planet. Chang. 2013, 100, 245–262. https://doi.org/10.1016/j.gloplacha.2012.10.008.
62. Razum, I., Hasan, O.; Brunović, D.; Schulz, H., Ilijanić, N.; Beg Paklar, G.; Ramisch, A.; Giaccio, B.; Šparica Miko, M.; Monaco, L., Miko, S. Influence of changing water mass circulation on detrital component and carbon burial of late Pleistocene and Holocene sediments in the eastern-central Mid-Adriatic deep, Marine and Petroleum Geology. 2024. 167, 106985, https://doi.org/10.1016/j.marpetgeo.2024.106985.
63. Ilijanić, N. Clay minerals in lake sediments along the eastern Adriatic coast as proxies of environmental changes during Late Pleistocene and Holocene. Ph.D. Thesis, Faculty of Science, University of Zagreb, Zagreb, Croatia, 2014. [In Croatian].
64. Siani, G., Paterne, M., Colin, C., 2010. Late glacial to Holocene planktic foraminifera bioevents and climatic record in the South Adriatic Sea. J. Quat. Sci. 25, 808–821. https://doi.org/10.1002/jqs.1360.
65. Alley, R. B. Ice-core evidence of abrupt climate changes. Proceedings of the National Academy of Sciences. 2000. 97(4), 1331–1334. https://doi.org/10.1073/pnas.97.4.1331
66. Meyers, P. A.; Teranes, J. L. Sediment Organic Matter. In Tracking Environmental Change Using Lake Sediments Vol 2: Physical and Geochemical Methods; Last, W. M., Smol, J. P., Eds.; Kluwer Academic Publisher: Dordrecht, 2001; pp 239–269.
67. Dormoy, I., Peyron, O., Combourieu-Neboutb, N., Goring, S., Kotthoff, U., Magny, M., Pross, J. (2009): Terrestrial climate variability and seasonality changes in the Mediterranean region between 15 000 and 4000 years BP deduced from marine pollen records, Climate of the Past 5, 615–632. https://doi.org/10.5194/cp-5-615-2009
68. Strasser, M.; Anselmetti, F.S.; Fäh, D.; Giardini, D.; Schnellmann, M. Magnitudes and source areas of large prehistoric northern Alpine earthquakes revealed by slope failures in lakes. Geology. 2006, 34, 1005–1008. https://doi.org/10.1130/G22784A.1
69. Strasser, M.; Monecke, K.; Schnellmann, M.; Anselmetti, F. Lake sediments as natural seismographs: a compiled record of Late Quaternary earthquakes in Central Switzerland and its implication for Alpine deformation. Sedimentology. 2013, 60, 319–341. https://doi.org/10.1111/sed.12003
70. Hartman, G., Bar-Yosef, O., Brittingham, A., Grosman, L., Munro, N.D. Hunted gazelles evidence cooling, but not drying, during the Younger Dryas in the southern Levant. Proc. Natl. Acad. Sci. U.S.A. 2016. 113, 3997–4002. https://doi.org/10.1073/pnas.1519862113.
71. Bout-Roumazeilles, V.; Combourieu-Nebout, N.; Desprat, S.; Siani, G.; Turon, J.L.; Essallami, L. Tracking atmospheric and riverine terrigenous supplies variability during the last glacial and the Holocene in central Mediterranean, Clim. Past. 2013. 9, 1065–1087, https://doi.org/10.5194/cp-9-1065-2013.

72. Lugović, B.; Majer, V. Eruptivi Senjske drage (Vratnika) kod Senja (Hrvatska, Jugoslavija), Geološki vjesnik. 1983, 36, 157–181.
73. Mercone, D., Thomson, J., Croudace, I.W., Siani, G., Paterne, M., Troelstra, S. Duration of S1, the most recent sapropel in the eastern Mediterranean Sea, as indicated by accelerator mass spectrometry radiocarbon and geochemical evidence. Paleoceanography. 2000, 15 (3), 336–347. https://doi.org/10.1029/1999PA000397.
74. Tesi, T., A. Asioli, D. Minisini, V. Maselli, G. Dalla Valle, F. Gamberi, L. Langone, A. Cattaneo, P. Montagna, F. Trincardi. Large-scale response of the Eastern Mediterranean thermohaline circulation to African monsoon intensification during sapropel S1 formation. Quaternary Science Reviews. 2017, 159, 139–154, https://doi.org/10.1016/j.quascirev.2017.01.020.
75. Combourieu-Nebout, N.; Peyron, O.; Bout-Roumazeilles, V.; Goring, S.; Dormoy, I.; Joannin, S.; Sadori, L.; Siani, G.; Magny, M. Holocene Vegetation and Climate Changes in the Central Mediterranean Inferred from a High-Resolution Marine Pollen Record (Adriatic Sea). Clim. Past. 2013, 9 (5), 2023–2042. https://doi.org/10.5194/cp-9-2023-2013.
76. Kallel, N.; Paterne, M., Duplessy, J.C., Vergnaud-Grazzini, C., Pujol, C., Labeyrie, L., Arnold, M., Fontugne, M., Pierre, C. Enhanced rainfall in the Mediterranean region during the last sapropel event. Oceanol. Acta. 1997, 20, 697–712.
77. Magny, M.; Miramont, C.; Sivan, O. Assessment of the impact of climate and anthropogenic factors on Holocene Mediterranean vegetation in Europe on the basis of palaeohydrological records. Palaeogeogr. Palaeoclimatol. Palaeoecol. 2002, 186, 1-2, 47–59.
78. Zanchetta, G., Drysdale, R. N., Hellstrom, J. C., Fallick, A. E., Isola, I., Gagan, M. K., and Pareschi, M. T.: Enhanced rainfall in theWestern Mediterranean during deposition of sapropel S1: stalagmite evidence from Corchia cave (Central Italy), Quaternary Sci. Rev. 2007, 26, 279–286, https://doi.org/10.1016/j.quascirev.2006.12.003.
79. Meyers, P. A. Applications of Organic Geochemistry to Paleolimnological Reconstructions: A Summary of Examples from the Laurentian Great Lakes. Org. Geochem. 2003, 34 (2), 261–289. https://doi.org/10.1016/S0146-6380(02)00168-7.
80. Morellón, M.; Anselmetti, F.S.; Ariztegui, D.; Brushulli, B.; Sinopoli, G.;Wagner, B.; Sadori, L.; Gilli, A.; Pambuku, A. Human-Climate Interactions in the Central Mediterranean Region during the Last Millennia: The Laminated Record of Lake Butrint (Albania). Quat. Sci. Rev. 2016, 136, 134–152. https://doi.org/10.1016/j.quascirev.2015.10.043.
81. Francke, A.; Wagner, B.; Leng, M.J.; Rethemeyer, J. A Late Glacial to Holocene Record of Environmental Change from Lake Dojran (Macedonia, Greece). Clim. Past 2013, 9, 481–498. https://doi.org/10.5194/cp-9-481-2013.
82. Thienemann, M.; Masi, A.; Kusch, S.; Sadori, L.; John, S.; Francke, A.; Wagner, B.; Rethemeyer, J. Organic Geochemical and Palynological Evidence for Holocene Natural and Anthropogenic Environmental Change at Lake Dojran (Macedonia/Greece). Holocene. 2017, 27, 1103–1114. https://doi.org/10.1177/0959683616683261
83. Shotyk, W.,Weiss, D.; Appleby P.G.; Cheburkin, A.K.; Frei, R.; Gloor, M.; Kramers, J.D.; Reese, S.; Van der Knaap, W.O. History of atmospheric lead deposition since 12,370 14C yr BP recorded in a peat bog profile, Jura Mountains, Switzerland. Science, 1998, 281, 1635–1640.
84. Brännvall, M.L., Bindler, R., Emteryd, O.; Renberg, I. Four thousand years of atmospheric lead pollution in northern Europe: a summary from Swedish lake sediments, Journal of Paleolimnology. 2001, 25, 421–435.
85. Fortis, A. Saggio d'osservazioni sopra l'Isola di Cherso ed Ossero. Venezia, 1771, 1971.
86. Velde, B.; Meunier, A. The origin of clay minerals in soils and weathered rocks. Springer, 2008.
87. Barnhisel, R.I.; Bertsch, P.M. Chlorites and hydroxy-interlayered vermiculite and smectite. In: Dixon, J.B. & Weed, S.B. (ed.): Minerals in soil environments. 2nd edition, Soil Science Society of America, USA, 729–788. 1989.
88. Velde, B. Origin and mineralogy of clays: clays and the environment. Springer-Verlag, Heidelberg. 1995.
89. Durn, G., Ottner, F., Slovenec, D. (1999): Mineralogical and geochemical indicators of the polygenetic nature of terra rossa in Istria, Croatia, Geoderma 91, 125–150. https://doi.org/10.1016/S0016-7061(98)00130-X
90. Razum, I.; Rubinić, V.; Miko, S.; Ružičić, S., Durn, G. Coherent provenance analysis of terra rossa from the northern Adriatic based on heavy mineral assemblages reveals the emerged Adriatic shelf as the main

recurring source of siliciclastic material for their formation. Catena. 2023, 107083. https://doi.org/10.1016/j.catena.2023.107083

91. Durn, G.; Rubinić, V.; Wacha, L; Patekar, M.; Frechen, M.; Tsukamoto, S.; Tadej, N.; Husnjak, S. Polygenetic soil formation on Late Glacial Loess on the Susak Island reflects paleo-environmental changes in the Northern Adriatic area. Quat. Int. 2018, 494, 236–247. https://doi.org/10.1016/j.quaint.2017.06.072
92. Wacha, L.; Mikulčić Pavlaković, S.; Frechen, M.; Crnjaković, M. The loess chronology of the Island of Susak, Croatia. E G - Quat. Sci. J. 2011, 60/1, 153–169. doi: 10.3285/eg.60.1.11
93. Durn, G.; Wacha, L.; Bartolin, M.; Rolf, C.; Frechen, M.; Tsukamoto, S., Tadej, N.; Husnjak, S., Li, Y.; Rubinić, V. Provenance and formation of the red palaeosol and lithified terra rossa–like infillings on the Island of Susak: a high–resolution and chronological approach. Quat. Int. 2018, 494, 105–129. https://doi.org/10.1016/j.quaint.2017.11.040